



Probabilistic assessment of climate-related impacts and risks in ports

D. Lucio^{*}, J.L. Lara, A. Tomás, I.J. Losada

IHCantabria - Instituto de Hidráulica Ambiental de la Universidad de Cantabria, Santander, Spain

ARTICLE INFO

Keywords:

Ports
Coastal structures
Critical infrastructures
Climate risks
Compound risks

ABSTRACT

Port activities are crucial for sustained, long-term economic growth, serving as the primary nodes for importing and exporting goods within global supply chains. Given their coastal locations, ports are inherently exposed to climate hazards, such as waves and extreme sea levels, requiring large investments in resilient infrastructure. This study introduces an innovative methodology for assessing climate-related impacts and risks in ports, applicable to both existing and new constructions. This approach aims to facilitate climate-informed decision-making and enhance the management of coastal structures and ports under high uncertainty. The methodology's novelty resides in: (1) the development of a port-specific risk framework capable of estimating impacts from both extreme events and daily conditions; (2) the integration of the latest advancements in nearshore climate hazard modeling; (3) the application of high-resolution tools for accurately simulating wave propagation towards harbor basins and the interaction between waves and structures; (4) the probabilistic determination of failure modes and operational shutdowns susceptible to climate conditions; and (5) the estimation of economic losses resulting from diminished operational capacity, in addition to the degradation of reliability and functionality in port infrastructures. Formulated within the Intergovernmental Panel on Climate Change (IPCC) risk framework and anchored in established Spanish Recommendations for Maritime Works (ROM Program), this methodology has been applied to a complex, state-owned, newly-built outer port in the Mediterranean Sea. Preliminary findings suggest that, over the course of a 50-year lifespan, climate-related risks could lead to cumulative losses nearing 10 million euros for such infrastructure. Nevertheless, in scenarios marked by extreme events, potential losses could escalate to as much as 100 million euros, despite their occurrence being relatively rare (with a probability of only 0.1%). It stresses the significant uncertainties encountered when evaluating climate-related risks for critical infrastructure, including ports, and highlights the critical need for advanced methodologies to accurately understand these risks.

1. Introduction

Ports are crucial for bolstering economies and ensuring the smooth operation of global supply chains. With around 3700 maritime ports worldwide, their role in facilitating trade and commerce on both local and global scales is indispensable [1]. As the main junctions for maritime transport, which carries approximately 80% of global trade by volume and more than 70% by value [2], ports are vital. Ocean freight, according to the Bureau of Transportation, constitutes 53% of EU imports, and the waterborne economy significantly contributes – about \$1777 billion annually – to the EU. Nevertheless, their strategic locations along rivers and coastal areas make them vulnerable to climate extremes and natural hazards, such as severe storms or cyclones. Remarkably, about a third of the world's ports are in regions prone to tropical storms [3], frequently exposing them to such risks. Assessing climate impacts and risks on coastal infrastructures, which are crucial for maintaining the safety and efficiency of port operations, becomes paramount. Ports, as critical infrastructures situated

in low-lying coastal zones, rely extensively on coastal structures to ensure their reliability, functionality, and operability. This research aims to examine the effects of climate conditions on the performance of these critical infrastructures, focusing on disruptions to coastal structures. The study will address the following questions: Q1: Assessing the performance of coastal infrastructure: Is it safe, functional, and operational? What safety and operating margins are available?; Q2: Identifying vulnerabilities: Which failure and stoppage modes are most susceptible to climate dynamics?; Q3: Evaluating climate-related impacts and risks: Which assets and operations are most at risk from climate-induced impacts?; Q4: Understanding climate-related impacts and risks: What are the potential effects on the reliability, functionality, and operability of port infrastructures, including associated uncertainties?; Q5: Addressing challenges: How can we ensure an equitable distribution of resources between public and private sectors to address these challenges?

^{*} Corresponding author.

E-mail address: david.lucio@unican.es (D. Lucio).

Coastal structure analysis distinctively evaluates impacts arising from daily or weather conditions, leading to operational disruptions, and from extreme events, which compromise reliability and functionality. Notably, frameworks such as the Spanish Recommendations for Maritime Works [4–6], alongside reports by The World Association for Waterborne Transport Infrastructure (PIANC), delineate criteria for assessing the Operational Limit State (OLS), Serviceability Limit State (SLS), and Ultimate Limit State (ULS). These distinctions pave the way for analyses centered solely on port operability (OLS) or a combined focus on port functionality and reliability (SLS and ULS, respectively) across various spatial scales. The initial research gap addressed in this study involves the development of an integrated port-oriented impact methodology that combines elements from ULS-based, SLS-based, and OLS-based research. This methodological advancement is further warranted by the prevalent management models in large-scale ports. Predominantly, such ports use a landlord system, where the public port authority owns and regulates the infrastructure, while private operators manage commercial services [7,8]. An exemplary embodiment of this model is the Spanish Port System, which is state-owned [9,10], where port authorities invest in coastal structures and basins, generating income from operational taxes. This context emphasizes the necessity for a holistic approach that concurrently evaluates structural integrity and operational hazards [11,12].

This categorization has motivated prior research on port and coastal structures to focus predominantly on these three key areas: operability, functionality, and reliability. On the one hand, studies focusing on operability have investigated the effects of non-operable climate conditions, such as increased wave agitation leading to shutdowns [13–15]. These analyses, ranging from local to port scales, project, for example, how future climate change could reduce port operability. Additionally, regional studies [16] have explored potential increased impacts due to higher wave overtopping rates [17,18] and wave heights within port basins [19]. On a global scale, the study by Izaguirre et al. [20] identifying port risks is notable. On the other hand, works oriented towards reliability and functionality aim to quantify structural impacts under extreme conditions. For example, Burcharth et al. [21] conducted a desk study on upgrading coastal structures to address increased wave loading and wave overtopping. Galiatsatou et al. [22], expanded this by incorporating economic optimization to manage the expected reduction in rubble mound breakwaters' reliability. Suh et al. [23] examined the progression of climate change-induced sliding failure in caisson breakwaters. Furthermore, while deterministic and probabilistic approaches have been applied to assess both operability, functionality and reliability impacts [21,24–27], probabilistic methods are preferred to handle high uncertainty. To address such uncertainty, significant emphasis has been placed on modeling compound climate conditions, considering their stochastic, multivariate, and non-stationary nature [28–31]. Then, this study aims to address a second research gap by integrating recent advancements in climate characterization to evaluate expected climate-related impacts and risks on coastal and port infrastructures.

Within such a context, the scientific community has developed a broad spectrum of methodologies for assessing impacts across various spatial scales and coastal scenarios, amidst prevailing uncertainties [32–34]. As previously described, the evolution of risk frameworks over recent decades has been significantly influenced by the study of climate change-induced impacts, with the Intergovernmental Panel on Climate Change (IPCC) risk framework serving as a pivotal Ref. IPCC [35]. This framework is esteemed for its versatility, offering applicability to a diverse range of natural and anthropogenic systems, including port and coastal infrastructures. It facilitates a comprehensive analysis by delineating: (1) the services and infrastructures at risk, (2) their vulnerability or capacity to withstand adverse impacts, and (3) the potential climatic hazards they face. By leveraging the IPCC framework, this study aims to pioneer a nuanced, port-oriented risk assessment methodology, charting a path towards comprehensive climate resilience in port and

coastal management. Although it is motivated for facing future climate challenges, it is intended to be applied to any stage of the coastal infrastructure lifespan. Then, the objective of this new framework is to evaluate climate-induced consequences comprehensively, supporting informed decision-making processes in the realms of coastal and port structure design, management, and adaptation to climate change.

A thorough search of the relevant literature detected there are not methodologies that allows assessing simultaneously risks arisen both from daily (non-operable climate conditions) and extreme events. Recognizing the critical importance of these infrastructures and the urgent need to assess climate-related impacts and risks, this research presents a novel framework for that. Then, the objective of this new framework is to evaluate climate-induced consequences comprehensively, supporting informed decision-making processes. Indeed, the framework is conceived to support decision-making under large uncertainty. In this context, particular attention should be given to the cascade of uncertainty [31], which underscores the necessity of propagating uncertainties from global or regional-scale climate modeling to the evaluation of climate-induced impacts and associated risks [36]. At its core, this framework amalgamates the established Spanish Recommendations for Maritime Works (ROM Program) with the structured risk assessment approach outlined by the Intergovernmental Panel on Climate Change [35]. By merging these two distinct yet complementary approaches, it strives to create a unified methodology that benefits from both the nuanced insights of Spanish expertise in coastal engineering and the global applicability of the IPCC's risk framework. While this framework has been tailored to suit the specific context of Spanish ROM program, it is important to note that it has a global applicability, making it adaptable to various international codes of practice. Furthermore, the methodology employed within this framework can be seamlessly integrated with other technical manuals and guidelines to enhance its versatility and effectiveness.

This study is structured as follows: Section 2 presents the methodology proposed for assessing the potential impacts and risks of climate hazards on ports, utilizing a probabilistic approach. Section 3 elaborates on this methodology through its application to a case study located on the Spanish coast, providing a detailed examination of the approach in a real-world context. The final section offers a discussion on the findings, drawing conclusions about their implications for stakeholders and the strategic planning of port operations.

2. Methodology

This investigation introduces an innovative tailored framework to address climate-related impacts on coastal and port structures following a high-resolution and probabilistic approach at the local scale. Following a comprehensive review of the existing literature, the framework is developed to quantitatively evaluate the anticipated consequences resulting from compound wave and sea-level hazards being the main objective to infer expected reliability, functionality and operability issues under high uncertainty. The methodology is formulated under the IPCC risk framework [35] and it is based on the usual failure and disruption mechanisms defined in port engineering (i.e. [5,6,37]).

The methodology can be organized into two main parts. The first concerns the characterization of the port system according to the needs of the goals of the risk assessment. The second entails the adaptation of the Intergovernmental Panel on Climate Change (IPCC) framework to the probabilistic assessment of climate-related impacts and risks in ports. Both parts are described in the following.

2.1. Definition of the Operational Unit concept: Bridging the gap between civil engineering design and port's economic performance

The primary challenge in conducting a realistic high-resolution analysis of climate-related impacts and risks is to account for the entire range of variability in climate hazards, exposure, and vulnerability at

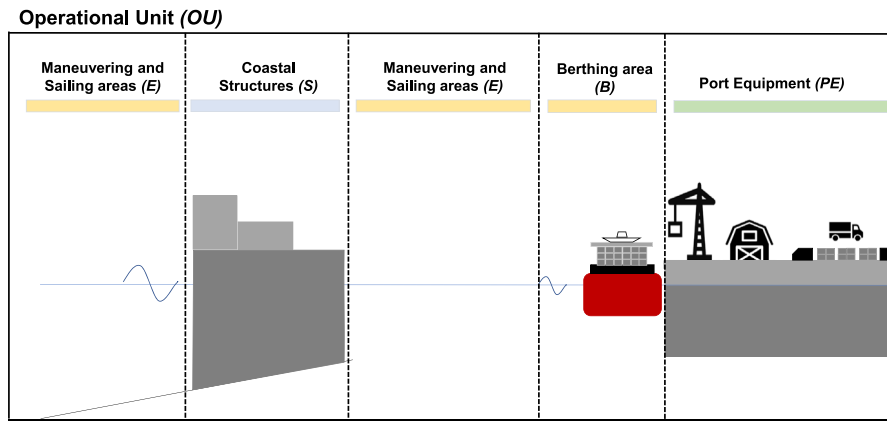


Fig. 1. Operational Unit (OU) scheme linking the structural, functional, and operational aspects of a specific port terminal.

the port scale. Concerning hazards, it is noteworthy how the wave climate varies along breakwater alignments and within harbor basins. For instance, when considering outer coastal structures designed to shield against extreme wave conditions, it becomes crucial to identify those coastal structure stretches most affected by extreme wave dynamics to pinpoint potential reliability and functionality issues that could impact port performance. Similarly, from an operational standpoint, it is relevant to determine which harbor basins, such as berthing areas, are most susceptible to wave agitation. When considering exposure, it is crucial to provide detailed descriptions of coastal structure features, including breakwater typologies and cross-section definitions, as well as their spatial location within harbor basins. Additionally, it is essential to identify the port equipment required for conducting port activities, such as cranes and storage buildings. It connects with the vulnerability description by establishing tolerable states for all exposed assets in response to climate dynamics.

While accounting for the heterogeneity of risk factors at the port scale is challenging, the primary obstacle lies in harmonizing traditional engineering practices with economic perspectives in risk analysis. As explained in the Introduction, civil engineering design is divided into three Limit States: Ultimate Limit State (ULS) related to the fulfillment of the design safety requirements; Serviceability Limit State (SLS) linked to functionality requirements; and Operational Limit State (OLS) associated to operability requirements. ULS and SLS are assessed by calculating the probabilities of failure, denoted as $P_{f,ULS}(ROM)$ and $P_{f,SLS}(ROM)$, respectively. In contrast, OLS requires the computation of operational-based indexes, such as the annual operability index denoted as $OPER(ROM)$. These Limit States are evaluated by isolating homogeneous units at the port scale, considering both the spatial component and the nonlinear interaction of climatic hazards and exposed elements. This approach has been extensively applied in coastal structures to verify their structural performance, involving the subdivision of breakwater alignments into subsets [38]. More recently, Campos et al. [14] extended the same approach to operational requirements by identifying Areas of Operational Interest (AOIs) to assess the operability of harbor basins, including berthing and sailing vessel areas. This approach allows for the analysis of port performance using reliability- and operational-based methods within the context of uncertainty [15].

In addressing the significant variability among exposed assets and port operations, each having varying vulnerability capabilities in dealing with climate hazards, the challenge is to transition from the previously described purely technical-based criteria to a comprehensive risk-based analysis that incorporates port management strategies [39]. To integrate both technical and governance aspects, here a new concept denoted as Operational Unit (OU) is presented. An Operational Unit can be defined as a set of homogeneous and independent port entities where specific cargo typologies are handled safely and efficiently (see

Fig. 1). These Operational Units encompass uniform elements within the coastal infrastructure that contribute to safety and efficiency, such as coastal structures, port equipment, and sea & land Areas of Operational Interest (AOIs). It is noteworthy that AOIs serve as operational areas within a particular Operational Unit (OU) in the same manner that coastal structures provide protection against wave action for that OU. Due to its operation-based nature, the movement of each cargo typology within the port must be precisely defined.

The concept of Operational Units within a coastal infrastructure aims to isolate sources of economic benefits and losses, allowing for a high-resolution analysis of climate-related impacts and risks that considers spatial, temporal, and profit variability at the port scale. As illustrated in Fig. 1 with the example of a container ship, an Operational Unit (OU) consists of *S* Coastal Structures, *PE* Port Equipment, *B* Berthing AOIs, and *E* Maneuvering and Sailing AOIs. Consequently, the risk framework is developed and implemented at the OU scale, while the overall risk for the entire port can be calculated as the sum of the risks associated with individual Operational Units (OUs).

2.2. Implementation of the new impact and risk framework

The implementation of the new methodology is formulated building on the Operational Unit (OU) concept. Subsequently, the framework is conceived at the OU scale. Nevertheless, the assumption of treating these Operational Units (OUs) as homogeneous and autonomous port entities enables the assessment of climate-related risks as the summation of individual risks.

In this research, a high-resolution and probabilistic approach is employed following Monte Carlo technique in order to characterize impact and risk indicators by the real probability distribution functions. While it may pose challenges in terms of complexity and data requirements, it yields more realistic results with a moderate to low residual uncertainty. Furthermore, the objective of this scientific contribution is to advance the state-of-the-art in assessing climate-induced consequences for a specific coastal infrastructure. The implementation of this approach follows a step-by-step process as outlined below. Concerning hazard characterization, reliable databases serve as sources of climate information, including hindcast and observational databases, as well as high-resolution climate change projections. Firstly, it is accomplished by downscaling offshore databases to the local scale to obtain high-resolution climate data tailored to site-specific conditions. Secondly, in the context of verifying the current or future design performance, advanced statistical techniques, such as multivariate copula functions, are employed to estimate climate conditions with a low probability of occurrence. Concerning exposure, maritime and navigation infrastructure (i.e., coastal structures, port equipment and maneuvering, sailing and basin areas) are characterized. It aligns with the definition of vulnerability, which is characterized as the susceptibility of any coastal

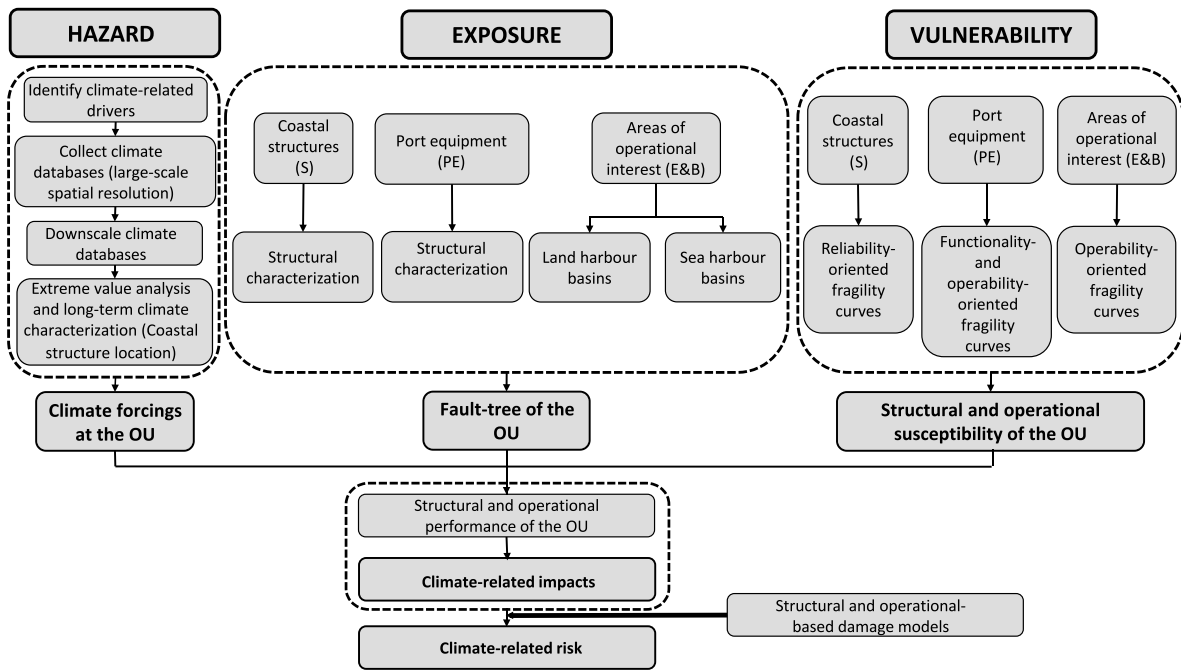


Fig. 2. Proposed methodology for assessing climate-related impacts and risks based on the Operational Unit (OU) concept.

infrastructure asset to be influenced by climate dynamics. In accordance with the Spanish Recommendations for Maritime Works (ROM Program), it is imperative that these assets adhere to design criteria that are contingent upon their socio-environmental and economic significance. Consequently, vulnerability is delineated by Ultimate Limit State (ULS), Serviceability Limit State (SLS) or Operational Limit State (OLS) technical design criteria, serving as indicators that demarcate thresholds distinguishing between safe/unsafe, functional/unfunctional, and operational/non-operational performance states.

As a result of characterizing risk terms in this manner, a high-resolution and probabilistic impact assessment is conducted. The main advantage of this approach is that it comprehensively accounts for the entire range of uncertainty related to climate–infrastructure interactions. This results in the generation of a probability density function that describes these impacts. This is particularly noteworthy because it provides the margin of safety under specific climate conditions, rather than solely indicating compliance with Limit States. As illustrated in [31], a crucial aspect of this research is the meticulous management of uncertainty. This entails a systematic propagation of uncertainty from hazard characterization, achieved through an appropriate downscaling strategy and multivariate extreme value analysis, to the impact assessment, utilizing tailored numerical models or semi-empirical formulas. It is retained until the final step of the methodology, which is dedicated to valuing the economic consequences derived from the previous impact assessment. Similar to the results oriented towards Ultimate Limit State (ULS), Serviceability Limit State (SLS), and Operational Limit State (OLS) risk indicators are expressed in terms of the probability of occurrence of adverse conditions, represented by their associated probability density functions. The overall methodology described here is shown in the flowchart in Fig. 2. Details on how it can be applied at high spatial resolution at Operational Unit (OU) scale is explained in the following.

2.2.1. Exposure definition

Exposure encompasses port facilities and operations located within a specific Operational Unit (OU) that could potentially be adversely affected by climate-related drivers. Addressing the challenges identified in this research, an accurate multi-exposure description involves dealing with the heterogeneity of exposed elements. Therefore, a detailed

characterization of port assets and operations is initially conducted. It should encompass coastal structures, port equipment (including cranes, cargo handling installations, warehouses, buildings, and land infrastructures like railways and roadways), as well as Areas of Operational Interest (AOIs).

Coastal structures can be structurally assessed from both stability and functionality perspectives using two-dimensional vertical (2DV) or three-dimensional (3D) models. While 2DV analyses are based on profile definitions, 3D studies incorporate layout information. Depending on the impact models employed to assess their hydraulic response, exposed coastal defenses can be characterized by cross-sections or fully 3D models. It is important to note that both models inherently include geometrical and structural uncertainties. With regards to Areas of Operational Interest (AOIs), these are defined by 2DH layouts (location and spatial extension) and a comprehensive description of the cargo typology, including dimensions, load conditions, and operational procedures.

The relationships between these exposed elements within a specific Operational Unit (OU) and the various underlying disruptive mechanisms related to reliability (ULS), functionality (SLS), and operability (OLS) are represented using a fault tree [40]. In this research, the fault-tree definition is extended from a single element such a cross-section of the breakwater to the distinguishing characteristics of an entire OU of a coastal infrastructure as shown in Fig. 3. This approach begins by defining the design limit states, which encompass safety, serviceability, and operability requirements [5]. Then, the disruptive mechanisms that may lead to the non-fulfillment of the technical requirements are described. Structural-induced mechanisms can trigger Failure Modes (FMs) [25,26], while Stoppage Modes (SMs) [14,15] can be attributed to operational reasons. This means that Ultimate Limit State (ULS) is analyzed by N Failure Modes (FMs), represented as $N1$ sub-mechanisms, which can cause the complete disruption of port activity due to a lack of structural safety. For instance, the Failure Mode (FM) “Damage to a caisson breakwater” can be triggered by sub-mechanisms like sliding and/or overturning. Serviceability Limit State (SLS) is evaluated by L Failure Modes (FMs), represented as $L1$ sub-mechanisms, which can cause temporary disruptions of port activity without affecting its structural safety. For example, the Failure Mode (FM) “Damage to port equipment” can be caused by sub-mechanisms

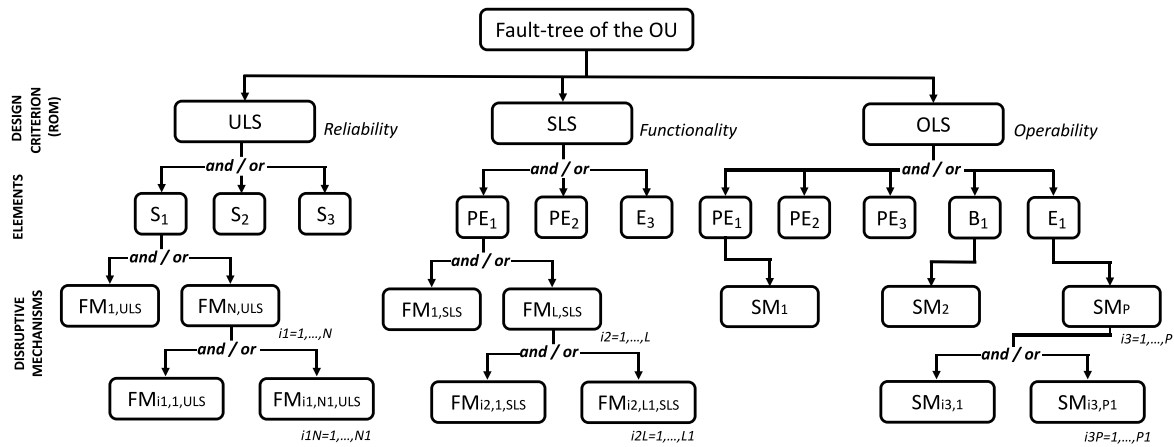


Fig. 3. Extended fault-tree of a certain OU.

such as excess mean overtopping discharge and/or maximum overtopping volume. Finally, Operational Limit State (OLS) is assessed by P Stoppage Modes (SMs), represented as $P1$ sub-mechanisms, which can cause temporary disruptions of port activity. In contrast to the ULS- and SLS-related Failure Modes (FMs), a Stoppage Mode (SM) ends as soon as the hazard ceases. Regarding the relationships and interactions between failure/stoppage modes, their performance can be conceptualized as a series or parallel system. In a series system, a failure/downtime occurs if any of the FM/SM takes place (*Or-gates* in Fig. 3). In contrast, a parallel system requires all FMs/SMs to occur simultaneously (*And-gates* in Fig. 3).

2.2.2. Vulnerability characterization

Vulnerability is defined as the proneness of the above described port facilities and operations located in a certain Operational Unit (OU) to be adversely affected by the climate-related physical drivers. For this purpose, fragility curves [41,42] are proposed. A fragility curve is a statistical function representing the probability of exceeding a given performance state of a FM/SM of an exposed element as a function of the external climate drivers and structural/geometrical parameters. Building the fragility curve $F(\Psi)$ of any exposed element consist of characterizing the governing parameter Ψ of the studied disruptive mechanism and its related performance states $\Psi_{threshold}$ (Fig. 4). Note that the term performance state can be associated to structural and operational disruptive reasons and it is characterized by a probability density function $f_{\Psi_{threshold}}(\Psi)$. It intends to address the stochastic nature of the vulnerability assessment as a result of non-deterministic and time-dependent threshold variables. Furthermore, governing parameters describe the hydraulic interaction between the climate drivers and the response of the analyzed element.

Failure Modes (FMs) of a coastal structure are focused on their hydraulic stability, defining their fragility curves by means of a measure of its reliability (safety coefficients or damage parameters) and a design criterion (damage levels). Ductile Failure Modes (FMs) such as “*damage progression to the armor layer in rubble-mound breakwater*” allow intermediate damage states, see $F_2(\Psi)$ and $F_3(\Psi)$ in Fig. 4, [43,44], while fragile Failure Modes (FMs) such as “*stability of the crown-wall*” are governed by non-failure/failure states, see $F_1(\Psi)$ in Fig. 4. Similarly, fragility curves of port equipment and Areas of Operational Interest (AOIs) are defined by combining functionality and operability governing parameters with their related tolerable values. Some hazards such as wave overtopping can generate temporal disruptions with and/or without structural consequences. In such situations, ad hoc fragility curves have to include an accurate statistical characterization of both performance states. Finally, fragility curves of mechanisms based on environmental variables as governing parameters directly relates its intensity to the probability of exceeding a performance state (i.e. wave agitation assessed by the significant wave height).

2.2.3. Hazard characterization

Concerning hazard characterization, the aim is to obtain compound wave and sea-level events tailored to site-specific coastal infrastructure conditions. According to Zscheischler et al. [45], compound events are defined as the combination of multiple drivers and/or hazards that contributes to societal or environmental risk. Then, compound events include (1) preconditioned event, (2) multivariate events, (3) temporally compound events (also referred as sequential events), and (4) spatially compounding events (also referred as concurrent event) as explained in [46]. In this context it is worth recalling coastal infrastructures like ports, breakwaters or coastal protections represent highly localized coastal interventions and, in most cases, due to their limited spatial scale, design, performance or operation conditions are based on climatic information on a very limited number of points or even only one depending on the infrastructures’ dimensions. Subsequently, in the context of coastal infrastructures, compound events adhere to the second definition (multivariate events). These events are conceptualized as the combination of waves, storm surges, tides, and sea-level rise, all contributing to coastal risks at a specific coastal infrastructure site.

Then the objective is twofold. Firstly, downscaling offshore climate data to the local scale. Secondly, characterizing both compound extreme events, as climate conditions triggering structural issues, and compound weather conditions, as climate conditions inducing port inoperability. The procedure related to hazard characterization consists of the following four steps. The first step is to identify the climate-related drivers that induce failure or non-operable conditions in coastal infrastructure. Once these are identified, the second step consists of collecting reliable offshore climate databases. Nevertheless, the scientific challenge is characterizing compound climate conditions, both including extreme and non-extreme, tailored to the particular coastal infrastructure conditions at any stage of its lifespan. This is achieved at the third and fourth steps, with special mention to extreme value analysis. Most of the current and more sophisticated works concerning multivariate extreme analyses take copula methods [47,48] as a powerful technique to describe the statistical dependence between the explanatory variables of a certain climate driver as well as driver-to-driver relationships. As a result, low-probability-high-impact events can be explored with a high level of accuracy. Copula-based framework has been applied using nested copulas [28,49,50], autoregressive models [51] or climate-dependent models [30,31,52,53]. However, these methods are based on information at offshore locations where wave transformation processes are not relevant to climate dynamics. Therefore, the proposed high-resolution methodology requires both taking into account simultaneity of hazards and the complex transformation processes at port-scale. This is a key aspect for properly assessing climate impacts and risks in coastal infrastructures over time, where (1) hazardous conditions are spatially correlated and (2) local wave

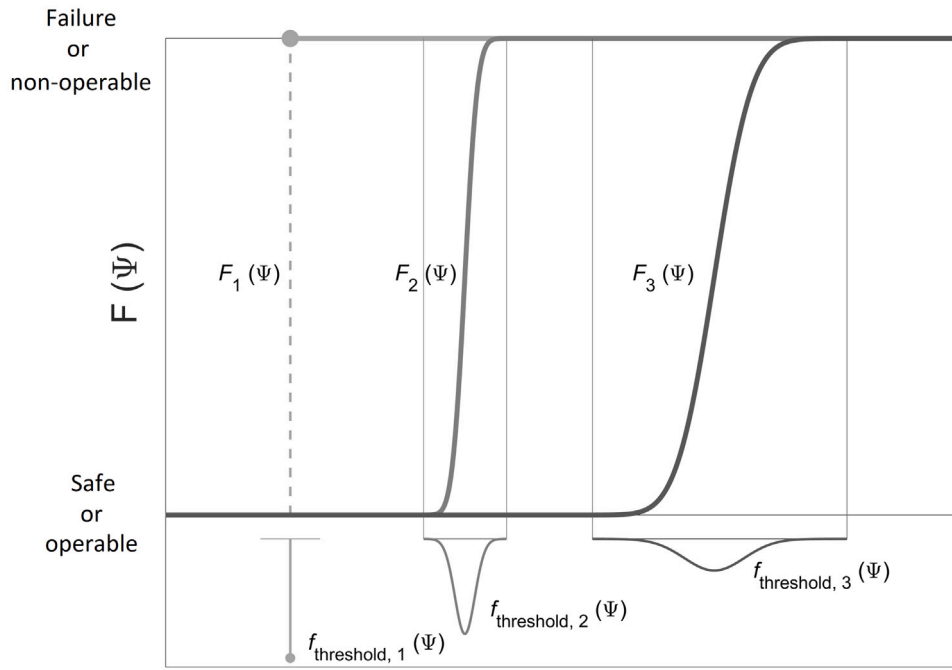


Fig. 4. Vulnerability characterization. Three categories of fragility curves, $F(\Psi)$, characterized by uncertainty in differentiating between safe and failure performance states.

transformation such as wave diffraction inside harbor basins plays a primary role. To overcome these issues, step three and four are jointly applied. First, some of these advanced statistical techniques are applied prior to their complex physical transformation phenomena on a dataset resulting from a higher-order spatial-scale (step 2). Then, any climate condition at this location can be downscaled to a coastal infrastructure site. Following metamodel techniques [54–56], an affordable computationally and reliable downscaling procedure is performed by coupling statistical techniques and process-based models to realistically propagate waves to the coastal infrastructure location.

2.2.4. Impact modeling

Structural and operational interaction between climate conditions and exposed elements is assessed following a probabilistic approach via a Monte Carlo technique. It integrates thousands of realistic synthetic time-series of environmental dynamics, applying some of the above described emulation techniques, and a detailed description of the exposed elements with a certain level of vulnerability as well as their relationships and disruptive mechanisms. It integrates previously described hazard, exposure and vulnerability characterization to quantify structural and operational performance of the Operational Unit (OU). Below it is explained how to implement a probabilistic framework within a reliability, functionality and operability analysis.

In the field of port engineering, approaches to wave–structure interaction can be categorized into three categories: state-of-the-art Semi-Empirical Formulae (SEF), specific laboratory tests, or numerical modeling. SEFs are formulated as g impact functions, establishing an analytical relationship between climatic drivers and structural/geometrical variables to determine the governing parameter related to structural behavior Ψ . However, SEFs have limited applicability within a specific range. Physical model tests allow for the modeling of complex processes and their interactions with coastal structures. Experimental results can be used to calibrate or reformulate the SEFs described earlier. Additionally, numerical fluid–structure interaction solvers are a cost-effective way to simulate local processes. For instance, two-dimensional vertical (2DV) Navier–Stokes models (i.e., [57,58]) and three-dimensional (3D) Navier–Stokes models (i.e., [59]) reproduce wave-breaking, nonlinear wave transformation, wave overtopping, and wave-induced loads on coastal structures.

Using some of the impact models mentioned above, technical-based requirements can be verified by comparing the obtained results with vulnerability curves (from $f_{\text{threshold},1}(\Psi)$ to $f_{\text{threshold},2}(\Psi)$). An impact occurs if it exceeds the threshold value. In the case of Semi-Empirical Formulae (SEF) as a reference, they establish the interaction of specific wave and sea-level conditions with the coastal structure, characterized by its structural parameters. This quantifies its response through a governing parameter Ψ , describing the analyzed hydraulic mechanism (Eq. (1)). If this parameter exceeds the threshold value $\Psi_{\text{threshold}}$, these conditions are considered to trigger failure or shutdown. Taking the stability formulations in outer armors as a reference, SEFs relate climatic loading variables (wave height, wave period and sea-level) with the size of the units (D_{n50}), their density (ρ_{rock}), and slope ($\tan \alpha$).

$$SEF \equiv g \rightarrow \Psi = f(R, S) \rightarrow \Psi$$

$$= f(\text{Climate conditions}; \text{Structural parameters}) \quad (1)$$

$$\text{Failure/Stoppage} \iff \Psi > \Psi_{\text{threshold}}$$

Therefore, a coastal structure – or any of its individual components – will satisfy the technical design requirements if the critical value of Ψ_{crit} throughout its lifetime remains below the established threshold value of $\Psi_{\text{threshold}}$. To illustrate this, let us consider the damage to the outer armor layer of a rubble mound breakwater, which is characterized by the damage level S . The extreme event that induces the highest damage determines S_{crit} . However, determining this value is subject to (1) inherent uncertainty stemming from both climatic and structural parameters and (2) its hydraulic response. In other words, the maximum extreme event expected at the toe of the breakwater during its lifetime exhibits stochastic behavior. Therefore, it is necessary to characterize S_{crit} using a Probability Density Function (PDF) rather than a single value. This is achieved by generating thousands of synthetic extreme events and considering the probabilistic nature of the wave–structure interaction (uncertainty of the Semi-Empirical Formulae SEF). This approach is applicable to any of the SEFs, which also provide confidence intervals for the proposed fits. By identifying the threshold value that separates the failure/non-failure region, the probability of failure P_f can be calculated to be expected as the area under the curve where $\Psi_{\text{crit}} > \Psi_{\text{threshold}}$. Following Monte Carlo approach, to achieve this, it is necessary to simulate multiple $U_{m,i}$ lifetimes to empirically approximate

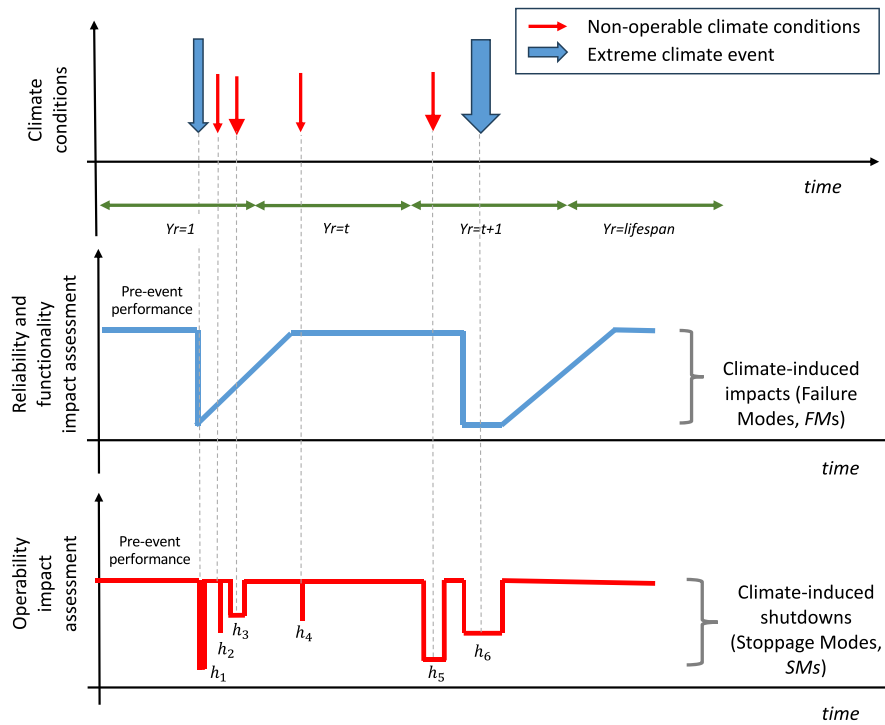


Fig. 5. Conceptual framework for evaluating economic consequences resulting from specific climate conditions (upper panel) leading to a loss of reliability or functionality (middle panel) or operability (lower panel).

the theoretical PDF of Ψ_{crit} . Then, the probability of failure resulting from approximating Ψ_{crit} through N_T synthetic lifetimes ($1 \leq U_{m,i} \leq N_T$), in which failure occurs in N_f of them, is calculated as follows:

$$P_f = \int_{g < 0} g(R, S) dr ds \rightarrow P_f = \int_{\Psi_{crit} > \Psi_{threshold}} PDF(\Psi_{crit}) d\Psi_{crit} \approx \frac{N_f}{N_T} \quad (2)$$

2.2.5. Risk assessment

The final step in the coastal risk assessment methodology involves translating the probabilistic impact-based results into probabilistic economic consequences. This involves addressing the economic valuation of consequences related to both Failure Modes (FMs) and Stoppage Modes (SMs), and it is achieved through the use of what are known as damage models [60,61]. A damage model is designed to estimate the economic costs or losses associated with various types of damage or disruptions. In the context of analyzing coastal infrastructures, these damages are primarily associated with extreme climate conditions that lead to structural failure, resulting in the loss of reliability and/or functionality (structural-based damage models). Disruptions, on the other hand, refer to situations where climate conditions induce a shutdown of port activities, leading to a loss of port operability (operational-based damage models). It is worth emphasizing that the definition of Operational Units (OUs) plays a crucial role in this process, as it helps to isolate sources of revenue and losses within the analysis of coastal infrastructure. This enables the computation of the total risk by summing individual risks for each Operational Unit (OU), providing a comprehensive view of the economic implications of climate-related impacts.

Prior to extending the port-oriented impact assessment methodology to a risk analysis, it is necessary to categorize port risks. Focusing on natural hazards, port performance can be impacted from both structural and operational perspectives. It is illustrated in Fig. 5. Structural risks are associated with Failure Modes (FMs) related to Ultimate Limit State (ULS) or Serviceability Limit State (SLS) triggered by extreme climate

events. These climate-induced failures are characterized by the inability to restore pre-event performance once the climate action ceases, as damage to coastal infrastructure or port equipment has occurred. On the other hand, operational risks are connected to Stoppage Modes (SMs) associated with Operational Limit State (OLS) triggered by various climate conditions affecting port activities, resulting in a certain NOP non-operable hours. This encompasses both extreme events and non-operational climate conditions. These climate-induced shutdowns are characterized by the ability to fully restore pre-event performance once the climate action ceases.

Beginning with structural impacts, it is important to emphasize that these are typically triggered by low-probability but high-impact climate events. This motivates the development of an event-based methodology for assessing structural risks as shown in Eq. (3). Then, economic valuation of a single disruptive event V_i taking place in a certain t year of its lifespan U_m is proportional to the initial cost of the coastal infrastructure potentially damaged.

$$V_i(t) = \alpha I_0 \left(1 + r\right)^{t-1} \left[\frac{\text{€}}{\text{event}}\right] \quad (3)$$

where:

I_0 is the initial investment in coastal infrastructure, €.

α is the ratio of initial investment potentially damaged by an extreme event, $0 < \alpha < 1$.

r is the discount rate.

In the context of operability impacts, a continuous or process-based approach is employed. This approach differs from an event-based one, which focuses on assessing consequences triggered by individual events. Instead, the process-based approach emphasizes the assessment of risks that arise from day-to-day operations since non-extreme climate conditions can interrupt port activity without causing structural failures. As a result, operational risks are averaged over a one-year period, as shown in Eq. (4). Then, the economic valuation of port inoperability O_i during a given t year (where $1 < t < U_m$), is proportional to the

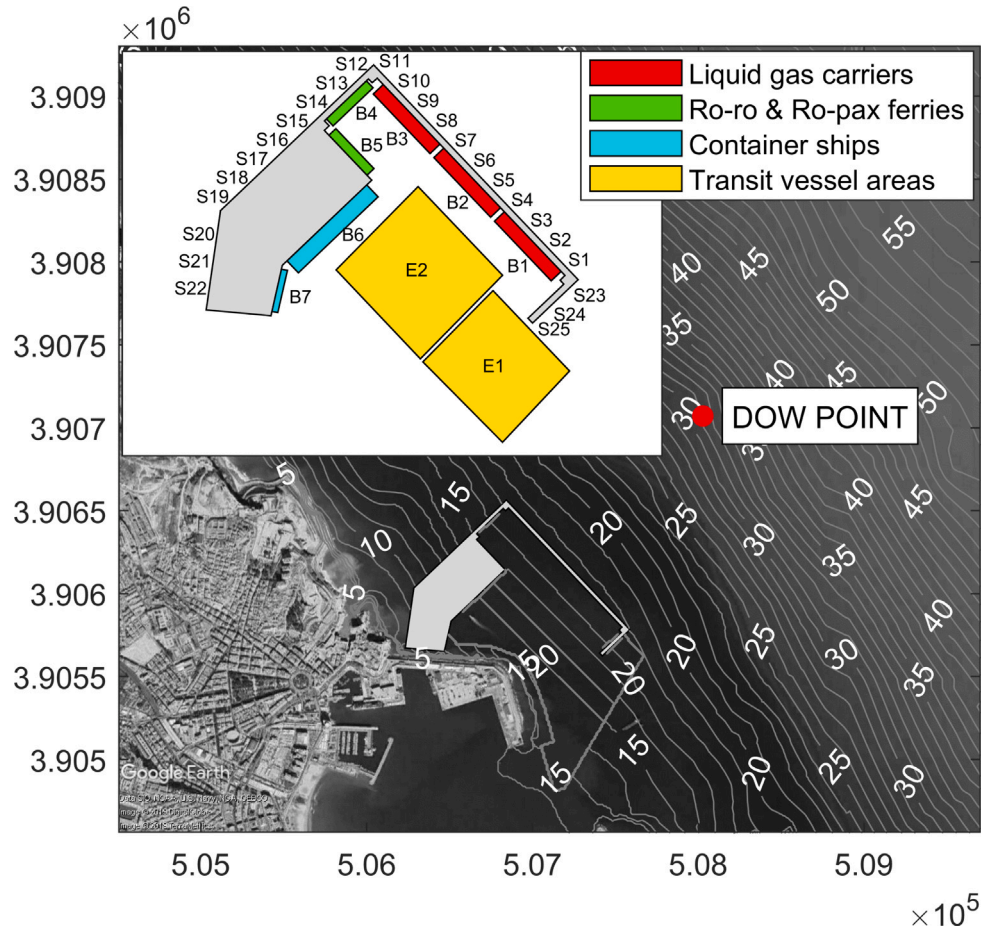


Fig. 6. Studied state-owned port of Melilla (Spain) with the bathymetry of the study area in meters. DOW point represents the location of the offshore hindcast database. A detailed spatial distribution of entrance waterways (E1 and E2), berthing areas (B1 to B7) and coastal structures (S1 to S25) are shown in the upper-left corner.

value of goods that cannot be handled due to non-operable climate conditions. Taking Fig. 5 as an example, the annual non-operability $NOP(t)$ during the first year is the sum of h_1 , h_2 , and h_3 .

$$O_i(t) = \underbrace{NOP(t)}_{\text{Non-operability, hours/year}} \underbrace{W_0(1+r_W)^{t-1}}_{\text{Projected demand, units/year}} \underbrace{C_0(1+r)^{t-1}}_{\text{Projected value €/unit}} \left[\frac{\text{€}}{\text{year}} \right] \quad (4)$$

where:

$NOP(t)$ Non-operable hours in a particular t year.

W_0 Goods handled at the coastal infrastructure in the first year of the analysis, units per year.

r_W growth rate of goods handled at the coastal infrastructure.

C_0 Value of goods handled at the coastal infrastructure in the first year of the analysis, € per unit.

r is the discount rate.

After applying an event-based approach for determining expected consequences triggered by compound extreme conditions and a continuous-time damage-based for quantifying expected operational consequences, structural and operational risks for any $U_{m,i}$ synthetic lifetime is obtained as shown in Eq. (5). By repeating the procedure for N_T synthetic lifetimes, the Probability Density Functions (PDFs)

for both expected structural and operational risks are obtained. It is highly interesting since it allows determining what is the probability of occurrence of a particular risk level (V_x or O_x) throughout the coastal infrastructure lifespan, as shown in Eq. (6). This is done to provide a probabilistic estimation of expected risks and to propagate inherent uncertainties from climate modeling to risk assessment within the context of this analysis.

$$V_{U_{m,i}} = \sum V_i \quad (5)$$

$$O_{U_{m,i}} = \sum O_i$$

$$Prob(V \leq V_x) = F_V(V_x) \quad (6)$$

$$Prob(O \leq O_x) = F_O(O_x)$$

3. Application to a case study: The new state-owned outer port of Melilla (Spain)

The study site is the new state-owned outer port of Melilla (Spain), in the Mediterranean Sea. Dealing with an expected traffic growth, attracting new port operators, reordering port areas and transferring the port activity outside the urban area are the main goals of the expansion project. As a result, the new multipurpose port shown in Fig. 6 is designed for the operation of liquid gas carriers, ro-ro & ro-pax ferries and container ships. Each of these cargo typologies uses common transit vessel areas (E1 and E2) and specialized berthing/mooring areas (from B1 to B7).

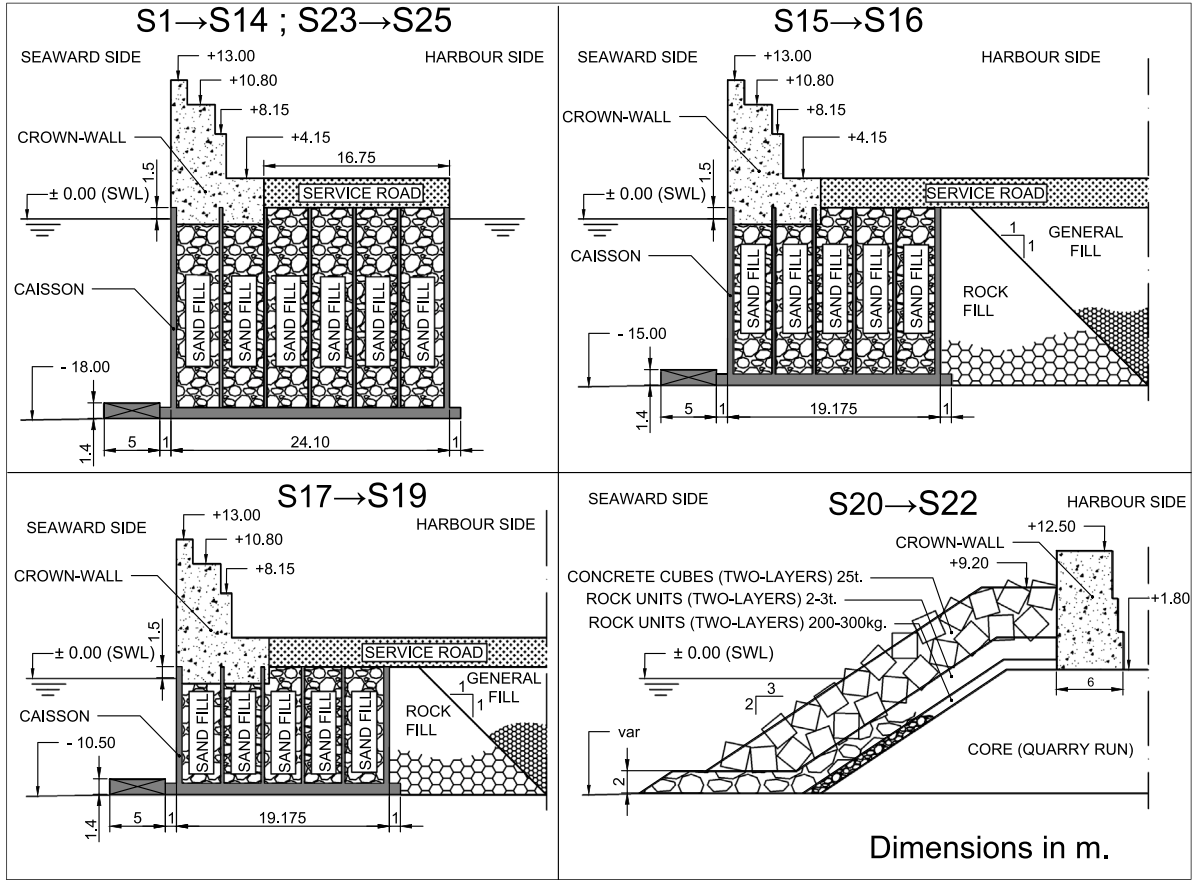


Fig. 7. Breakwater typologies defined by their cross-sections. S1 to S14 and S23 to S25; S15 to S16; S17 to S19 are composed by caissons varying progressively their width and height. S20 to S22 are built using a rubble-mound breakwater typology with concrete units (Dimensions in meters).

The proposed extension expands the port seawards by means of four breakwater alignments (Fig. 7), combining rubble mound (from S20 to S22) and vertical (from S1 to S19; and S23 to S25) breakwaters. According to ROM:1.0-09 [5], project requirements are defined by a minimum useful life of $U_m = 50$ years; a maximum joint probability of failure for the Ultimate Limit State (ULS) $P_{f,ULS}(ROM) = 0.10$; a maximum joint probability of failure for the Serviceability Limit State (SLS) $P_{f,SLS}(ROM) = 0.10$; and a minimum operability $OPER(ROM) = 0.95$. These are verified applying a Monte Carlo simulation method after synthetically generating $N_T = 1000$ lifetimes at hourly time-scale (438 million sea-states), which are taken from [30].

The first requirement of such framework is to identify Areas of Operational Interest (AOIs), coastal structures and port equipment belonging to each Operational Unit (OU). In this work, only sea AOIs are defined as a function of the vessel typology of the analyzed OU. It is especially relevant in areas used by several Operational Units (OUs) because a harbor basin may include different AOIs. A cross-section of the breakwater alignment is characterized every 100 m. Hence, it is accompanied by cranes and port buildings located on top of each cross-section, characterizing the port equipment PE of the Operational Unit (OU). PE is characterized by the cross-sections S to which it belongs since wave overtopping is the only Failure Mode (FM) assigned to the functionality analysis. As shown in Eq. (7) eleven OUs are obtained according to the revenue sources, vessel tracking, and vessel typology and breakwater typology. A detailed description on how to implement such methodology in OU1 can be found in Appendix A. In the following sections, climate-related impacts and risks will be computed for each

Operational Unit (OU) as well as for the entire coastal infrastructure.

$$\begin{aligned}
 &OU1 = E_1 | OU1 \cup E_2 | OU1 \cup B_1 \cup S_1 \cup S_2 \cup S_3 \cup S_4 \\
 &OU2 = E_1 | OU2 \cup E_2 | OU2 \cup B_2 \cup S_5 \cup S_6 \cup S_7 \\
 &OU3 = E_1 | OU3 \cup E_2 | OU3 \cup B_3 \cup S_8 \cup S_9 \cup S_{10} \cup S_{11} \\
 &OU4 = E_1 | OU4 \cup E_2 | OU4 \cup B_4 \cup S_{12} \cup S_{13} \cup S_{14} \\
 &OU5 = E_1 | OU5 \cup E_2 | OU5 \cup B_5 \\
 &OU6 = E_1 | OU6 \cup E_2 | OU6 \cup B_6 \\
 &OU7 = E_1 | OU7 \cup E_2 | OU7 \cup B_7 \\
 &OU8 = S_{15} \cup S_{16} \\
 &OU9 = S_{17} \cup S_{18} \cup S_{19} \\
 &OU10 = S_{20} \cup S_{21} \cup S_{22} \\
 &OU11 = S_{23} \cup S_{24} \cup S_{25}
 \end{aligned}
 \left. \begin{array}{l} \\ \\ \\ \\ \\ \\ \\ \\ \\ \\ \end{array} \right\} \begin{array}{l} E \cup B \cup S \\ \\ \\ \\ E \cup B \\ \\ S \end{array} \quad (7)$$

3.1. Exposure, vulnerability and hazard characterization

As it has been previously explained, exposure characterization starts by describing each Operational Unit (OU) system by an extended fault-tree. In this work, a series of wave and sea-level related hazards are the only physical events affecting the design requirements as summarized in Table 1. ULS-impacts are evaluated by the hydraulic stability of vertical or rubble mound breakwaters to deal with an excess of wave loading; SLS-impacts are assessed by the hydraulic capability of port equipment to resist an excess of projected wave overtopping over coastal structures; OLS-impacts by the capacity of cranes and Areas of Operational Interest (AOIs) to withstand an excess of wave overtopping

Table 1

Hazards driving impacts on port environment. Excess of wave loading is related to the ULS; excess of wave overtopping both to SLS & OLS; excess of wave agitation to OLS. For each hazard, the corresponding climatic drivers are identified.

	Excess of wave loading	Excess of wave overtopping	Excess of wave agitation
OU1	$S1, S2, S3, S4$	$S1, S2, S3, S4$	$E1 OU1, E2 OU1, B1$
OU2	$S5, S6, S7$	$S5, S6, S7$	$E1 OU2, E2 OU2, B2$
OU3	$S8, S9, S10, S11$	$S8, S9, S10, S11$	$E1 OU3, E2 OU3, B3$
OU4	$S12, S13, S14$	$S12, S13, S14$	$E1 OU4, E2 OU4, B4$
OU5	–	–	$E1 OU5, E2 OU5, B5$
OU6	–	–	$E1 OU6, E2 OU6, B6$
OU7	–	–	$E1 OU7, E2 OU7, B7$
OU8	$S15, S16$	$S15, S16$	–
OU9	$S17, S18, S19$	$S17, S18, S19$	–
OU10	$S20, S21, S22$	$S20, S21, S22$	–
OU11	$S23, S24, S25$	$S23, S24, S25$	–
Climatic drivers	$H_s, H_{max}, T_p, T_m, Dir, SWL, [Sea\ states\ sequence]$	$H_s, T_m, T_{m-1,0}, Dir, SWL$	$H_s, T_p, Dir, SWL, \gamma_{sea\ state}, \sigma_{sea\ state}$
Disruptive mechanisms	$FM_{1,ULS}, FM_{2,ULS}, FM_{3,ULS}, FM_{4,ULS}, FM_{5,ULS}$	$FM_{1,SLS}, FM_{2,SLS}, SM_{1,OLS}, SM_{2,OLS}$	$SM_{3,OLS}$

or wave agitation to carry out port operations. This implies that the full range of port impacts are assessed from OU1 to OU4; only operational impacts due to an excess of wave agitation are quantified from OU5 to OU7; and all, except operability due wave agitation, are evaluated from OU8 to OU11. The fault-tree is conceived as a series system. Exposed elements are characterized next. Coastal structures are studied by independent cross-sections (2DV models) as shown in Fig. 7. The rubble mound breakwater is located in the shallower area, consisting of an outer layer of 25 ton concrete cubes; a secondary layer with 2–3 tons rock units and a concrete crown-wall with a crest level at 12.50 m. Three different vertical breakwater cross-sections varying in width and height are also considered. Accordingly, the main vertical breakwater alignment is composed by caissons 24.1 m wide and 19.5 m high, with a concrete crown-wall lying on the cap with a crest level at 13.00 m. Areas of Operational Interest (AOIs) are characterized by the harbor basin area required for a given vessel typology to carry out port operations (entrance to the port, maneuvering or loading/unloading activities). Finally, wave-related disruptive mechanisms triggering a port impact are defined for each of the elements previously described. Failure Modes (FMs) assigned to Ultimate Limit State (ULS) refer to processes leading to a structural damage to coastal structures due to wave action. In this case study, we concentrate exclusively on hydraulic failure modes, which are identified as the predominant mechanisms contributing to a loss of structural safety. On the one hand, in vertical breakwaters, it is evaluated by means of the sliding and overturning stability of the caissons both under wave crest and trough conditions. On the other hand, rubble mound breakwater cross-sections are analyzed based on the damage to the outer concrete armor layer and the rigid body stability of the crown-wall. Serviceability Limit State (SLS) is quantified by the disruptive mechanisms of overtopping flows causing a structural damage to cranes and port buildings. At the end, the Stoppage Modes (SMs) related mechanisms which may induce port operations stoppage are wave agitation in AOIs and wave overtopping over coastal structures, respectively.

To further investigate whether the Failure Modes (FMs) and Stoppage Modes (SMs) take place, fragility curves are defined (Table 2). Sliding- and overturning-induced FMs are expressed as a ratio of the structural capability of the analyzed exposed element to wave loading. Using a traditional limit equilibrium method, a unit Safety Factor (SF) separates the failure/non-failure performance states. Ductile FMs associated with the damage to the outer concrete armor layer in rubble-mound cross-sections is evaluated by the well-established damage parameter N_{od} . As known, it relates the damage to armor layer to displaced armor units. In this work, three damage levels are studied according to design procedures [62]: initiation of damage (SD), Intermediate damage (ID) and failure (F). Wave overtopping, can be directly investigated by the mean overtopping discharge (q) and the maximum overtopping volume (V_{max}) following EurOtop [63]. Besides, it could be a cause of both a FM and SM. Consequently, each of

these two parameters, governing wave overtopping is described by two-performance states. Wave agitation is assessed based on wave height H_s over a certain Area of Operational Interest (AOI) as a function of the vessel typology. Because the resulting downtime/non-downtime performance states differ slightly from one design guideline to another, threshold values are statistically characterized by the ensembles of the limit operating conditions given in [64–66]. The resulting fragility curves for wave agitation are shown in Table 3. For instance, for the Area of Operational Interest (AOI) B4, a mean μ of 0.4 m and a standard deviation of σ 0.1 m are calculated from measurements of 0.4 m, 0.5 m, and 0.3 m, which are sourced from the aforementioned manuals. These fragility curves tend towards $F_2(H_s)$ or $F_3(H_s)$ (see Fig. 4) depending on the coefficient of variation ($CV = \sigma/\mu$, defined as ratio of the standard deviation σ to the mean μ). As can be observed, the remaining fragility curves are $F_1(\Psi)$ (Table 2).

The last item to be described is the compounding behavior of the identified wave-related hazards at the infrastructure site. For this purpose, a statistical-numerical hybrid downscaling technique presented by Camus et al. [67] is applied to propagate synthetic offshore databases (1000 realizations of 50 years at hourly time-scale) taken from [30]. After taking such synthetic database, synthetic climatic drivers (the significant wave height H_s ; the mean wave period T_m ; the peak wave period T_p ; the mean wave direction Dir and the storm surge SS) are homogeneously downscaled to port areas applying the metamodel strategy explained in [15]. It consists of (1) selecting a subset of sea states covering the wave climate variability in the synthetic database, (2) propagating the reduced subset to port areas, (3) reconstructing any simulated sea-state in any Operational Unit (OU). Following the above, 500 offshore marine conditions are selected applying the maximum dissimilarity algorithm [67] over the 4-dimensional data space $[H_s, T_p, Dir, SWL]$. Concerning the astronomical tide AT , it is independently characterized from the harmonic analysis of the global model of ocean tides TPX07.2 at hourly time-scale. The Still Water Level (SWL) is composed by the sum of SS and AT . Due to the low tidal range at the study location (<1.5 m), the influence of the sea-level on wave propagation is not considered. After that, the numerical model MSP [68] is applied to downscale the representative wave conditions from offshore location to inside the port. This model is based on the elliptical mild slope equations, solving the combined refraction–diffraction of water waves as well as the partial reflection of harbor boundaries in semi-enclosed basins. Because this work concerns both investigating wave heights inside harbor basins (Areas of Operational Interest) and coastal-structures (S), the reduced subset is simulated in two configurations. The first one is applied to simulate wave agitation, taking a reflection coefficient (K_r) equal to 0.85 in the vertical and 0.35 in the rubble-mound breakwater alignments, respectively. The second one is used to model the incident wave energy on coastal structures, considering fully-absorbing boundaries (K_r equals to 0) along the new port alignments. In both cases, the reflection coefficients adopted along

Table 2

Vulnerability characterization of each FM/SM related to the analyzed exposed elements. Each of these is described by the governing parameter explaining the studied mechanism as well as the statistical characterization of the performance states.

FM/SM	Governing parameter, Ψ	Performance states, $f_{threshold}(\Psi)$
$FM_{1,ULS}$: Sliding of the caisson	Safety Factor, $SF_{sliding}[-]$	$SF_{sliding,threshold} \sim N(\mu = 1; \sigma = 0)$
$FM_{2,ULS}$: Overturning of the caisson	Safety Factor, $SF_{overturning}[-]$	$SF_{overturning,threshold} \sim N(\mu = 1; \sigma = 0)$
$FM_{3,ULS}$: Damage to the outer concrete armor layer	Damage parameter, $N_{ad}[-]$	$N_{ad,SD} \sim N(\mu = 0.5; \sigma = 0)$ $N_{ad,LD} \sim N(\mu = 1; \sigma = 0)$ $N_{ad,F} \sim N(\mu = 2; \sigma = 0)$
$FM_{4,ULS}$: Sliding of the crown-wall	Safety Factor, $SF_{sliding}[-]$	$SF_{sliding,threshold} \sim N(\mu = 1; \sigma = 0)$
$FM_{5,ULS}$: Overturning of the crown-wall	Safety Factor, $SF_{overturning}[-]$	$SF_{overturning,threshold} \sim N(\mu = 1; \sigma = 0)$
Wave overtopping	$FM_{1,SLS}$ and $SM_{1,OLS}$: Mean overtopping discharge, $q [l/s/m]$	$q_{SLS,threshold} \sim N(\mu = 20; \sigma = 0)$ $q_{OLS,threshold} \sim N(\mu = 0.3; \sigma = 0)$
	$FM_{2,SLS}$ and $SM_{2,OLS}$: Maximum overtopping volume, $V_{max} [l/m]$	$V_{max,SLS,threshold} \sim N(\mu = 20,000; \sigma = 0)$ $V_{max,OLS,threshold} \sim N(\mu = 600; \sigma = 0)$
$SM_{3,OLS}$: Wave agitation	Significant wave height, $H_s [m]$	See Table 3

Table 3

Detailed fragility curves description for $SM_{3,OLS}$ according to the vessel typology of each OU.

	AOI	$f_{threshold}(H_s)$
OU1	$E1 OU1$	$H_{s,threshold} \sim N(\mu = 1.50 \text{ m}; \sigma = 0.45 \text{ m})$
	$E2 OU1$	$H_{s,threshold} \sim N(\mu = 1.50 \text{ m}; \sigma = 0.45 \text{ m})$
	$B1$	$H_{s,threshold} \sim N(\mu = 0.90 \text{ m}; \sigma = 0.17 \text{ m})$
OU2	$E1 OU2$	$H_{s,threshold} \sim N(\mu = 1.50 \text{ m}; \sigma = 0.45 \text{ m})$
	$E2 OU2$	$H_{s,threshold} \sim N(\mu = 1.50 \text{ m}; \sigma = 0.45 \text{ m})$
	$B2$	$H_{s,threshold} \sim N(\mu = 0.90 \text{ m}; \sigma = 0.17 \text{ m})$
OU3	$E1 OU3$	$H_{s,threshold} \sim N(\mu = 1.50 \text{ m}; \sigma = 0.45 \text{ m})$
	$E2 OU3$	$H_{s,threshold} \sim N(\mu = 1.50 \text{ m}; \sigma = 0.45 \text{ m})$
	$B3$	$H_{s,threshold} \sim N(\mu = 0.90 \text{ m}; \sigma = 0.17 \text{ m})$
OU4	$E1 OU4$	$H_{s,threshold} \sim N(\mu = 1.50 \text{ m}; \sigma = 0.45 \text{ m})$
	$E2 OU4$	$H_{s,threshold} \sim N(\mu = 1.50 \text{ m}; \sigma = 0.45 \text{ m})$
	$B4$	$H_{s,threshold} \sim N(\mu = 0.40 \text{ m}; \sigma = 0.10 \text{ m})$
OU5	$E1 OU5$	$H_{s,threshold} \sim N(\mu = 1.50 \text{ m}; \sigma = 0.45 \text{ m})$
	$E2 OU5$	$H_{s,threshold} \sim N(\mu = 1.50 \text{ m}; \sigma = 0.45 \text{ m})$
	$B5$	$H_{s,threshold} \sim N(\mu = 0.40 \text{ m}; \sigma = 0.10 \text{ m})$
OU6	$E1 OU6$	$H_{s,threshold} \sim N(\mu = 1.50 \text{ m}; \sigma = 0.45 \text{ m})$
	$E2 OU6$	$H_{s,threshold} \sim N(\mu = 1.50 \text{ m}; \sigma = 0.45 \text{ m})$
	$B6$	$H_{s,threshold} \sim N(\mu = 0.50 \text{ m}; \sigma = 0.20 \text{ m})$
OU7	$E1 OU7$	$H_{s,threshold} \sim N(\mu = 1.50 \text{ m}; \sigma = 0.45 \text{ m})$
	$E2 OU7$	$H_{s,threshold} \sim N(\mu = 1.50 \text{ m}; \sigma = 0.45 \text{ m})$
	$B7$	$H_{s,threshold} \sim N(\mu = 0.50 \text{ m}; \sigma = 0.20 \text{ m})$

the coastal area are $K_r = 0.05$ for dissipative beaches, $K_r = 0.35$ for rubble-mound breakwaters, $K_r = 0.60$ for cliffs and $K_r = 0.85$ for vertical breakwaters. Consequently, each of the 500 synthetic sea states is spectrally simulated twice following the highly efficient procedure described in [69] and [15]. Fig. 8 provides wave propagation maps for two representative storminess wave conditions in both configurations. As can be noted, the incoming waves inside the harbor basins are highly affected by the wave reflection in the existing port. Finally, the entire database is statistically reconstructed applying the 3-dimensional interpolation with radial basis functions [67]. Synthetic time-series at Areas of Operational Interest (AOIs) are obtained applying the wave agitation configuration results, and hourly sea states at coastal structures locations are derived from the incident wave energy configuration analysis. Fig. 9 shows the synthetic extreme incident significant wave height regime in each cross-section location for a 50-year return period. As can be observed, the largest values are obtained from S1 to S11 with a slight variation along this main vertical breakwater alignment. Besides, it is highly influenced by wave breaking as the water depth decreases.

3.2. Climate-related impacts assessment

The interaction between climate scenarios and exposed elements within an Operational Unit (OU) is assessed using a probabilistic approach through Monte Carlo techniques. This approach combines thousands of realistic synthetic time series of environmental dynamics with a detailed description of the exposed elements, their relationships, and disruptive mechanisms, as previously explained in the preceding sections. With the exposure, vulnerability, and hazard terms characterized for each Operational Unit (OU), climate-related impacts are assessed. The impact modeling of Failure Modes (FMs) and Stoppage Modes (SMs) is carried out by applying probabilistic Semi-Empirical Formulae (SEF). These can be found in Appendix B. SEF provides the value of the governing parameter Ψ , which describes the analyzed disruptive mechanism under specific environmental and structural conditions. A comprehensive non-deterministic modeling, taking into account the uncertainties associated with the SEF. This strategy is implemented through a three-step method.

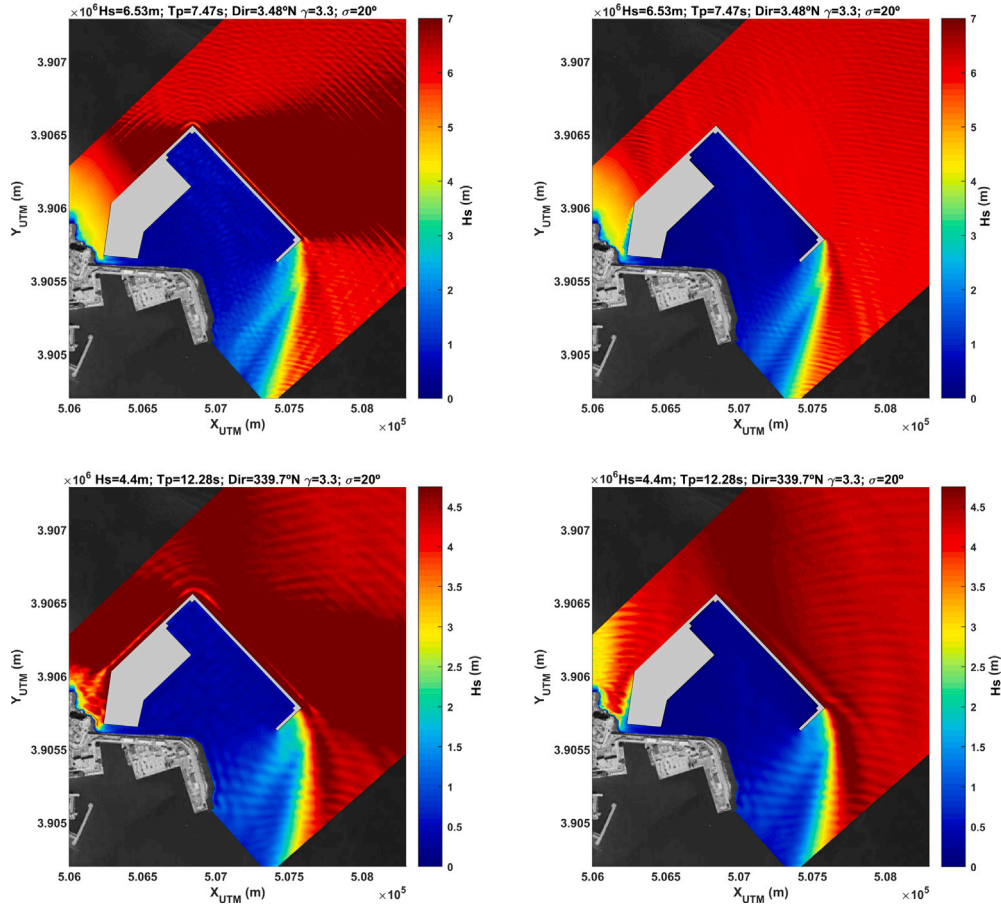


Fig. 8. Wave propagation modeling from the DOW point to port areas using the MSP numerical model for predominant north and north-northwest extreme wave conditions (upper and lower panels, respectively). 2DH significant wave height maps in left panels refer to wave agitation configuration, and right panels to incident wave height configuration.

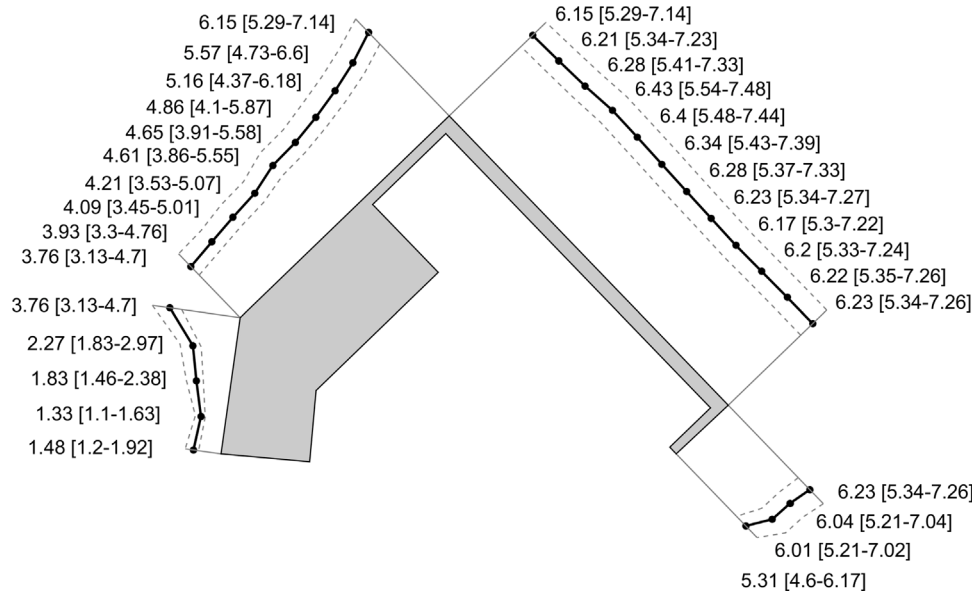


Fig. 9. Spatial extreme distribution of H_s along the new breakwater alignment for a return period of 50 years with 90% confidence interval based on the downscaled synthetic wave climate (1000 samples; H_s in meters).

1. Statistical characterization of the involved variables. 1000 samples of fifty-year long time series of climatic drivers are synthetically generated at hourly time-scale following the above-described method. Non-climatic drivers related to the resistance

properties of each cross-section are simulated for each life-time. To do this, the following breakwater-dependent parameters are assumed normally distributed [25,70] $N(\mu; \mu \times CV)$ as follows: mass density of the reinforced concrete components

- $\rho_{r-concrete}$ [kg/m³] $\sim N(2350; 2350 \times 0.02)$; mass density of the sand fill ρ_{sand} [kg/m³] $\sim N(1800; 1800 \times 0.05)$; mass density of the concrete components $\rho_{m-concrete}$ [kg/m³] $\sim N(2300; 2300 \times 0.02)$; mass density of the service road ρ_{road} [kg/m³] $\sim N(2000; 2000 \times 0.05)$; mass density of the rock fill ρ_{rock} [kg/m³] $\sim N(2000; 2000 \times 0.05)$; friction coefficient concrete-foundation δ_{c-f} [–] $\sim N(0.65; 0.65 \times 0.05)$; seaward slope $\tan \alpha$ [–] $\sim N(2/3; 2/(3 \times 0.05))$; angle of friction of rock fill ϕ_{rock} [°] $\sim N(45; 45 \times 0.05)$. As can be observed, the coefficients of variation CV range from 2 to 5%.
2. Probabilistic approach for the prediction of the structural and operational response to wave-related hazards. In vertical breakwaters, an excess of wave loading can trigger the sliding ($FM_{1,ULS}$) and/or overturning ($FM_{2,ULS}$) of the caisson. The Goda – Takahashi method [71] and [72] is applied for evaluating wave action on these cross-sections under Wave Crest conditions (WC), including the uncertainty and bias estimation of wave forces and moments. Wave pressure under Wave Trough conditions (WTh) is estimated following the formula developed by Sainflou [73] and Oumeraci et al. [74]. In relation to rubble-mound cross sections ($FM_{3,ULS}$), the damage parameter of the outer concrete armor layer is quantified as a function of time according to the cumulative damage procedure proposed by van der Meer [75]. Wave induced pressures on crown-walls ($FM_{4,ULS}$ and $FM_{5,ULS}$) are predicted following van Gent and van der Werf [76] in order to take the influence of wave obliqueness into account. Finally, in both cases, the probabilistic approaches proposed by EurOtop [63] are applied to evaluate overtopping rates ($FM_{1,SLs}$, $FM_{2,SLs}$, $SM_{1,OLS}$, $SM_{2,OLS}$).
 3. Probabilistic approach for the assessment of the structural and operational performance to wave-related hazards. Sliding and overturning Failure Modes (FMs) are evaluated by means of the previously described Safety Factor (SF). Note that from S15 to S19 the earth pressure due to the rock fill should be taken into account. Therefore, the passive and active land induced pressures on these caissons are also quantified applying Coulomb's method for wave crest and wave trough conditions, respectively. Fig. 10 shows the probability distributions for the minimum safety factors for vertical breakwaters OU-by-OU. These Probability Density Functions (PDFs) are computed based on the minimum Safety Factor (SF) values for each of the 1000 samples. As observed, the most hazardous conditions can be found for the sliding Failure Mode (FM) under wave crest conditions (SF near and below 1).

When analyzing the spatial distribution, it becomes apparent that the lowest values are obtained at the main breakwater alignment, spanning from OU1 to OU3. Moreover, the proposed high-resolution methodology offers a more detailed understanding of the less resilient cross-sections and the environmental conditions with the greatest disruptive potential (refer to Table 4). For example, consider the Operational Unit (OU) with the highest probability of failure for the ultimate limit state, $P_{f,ULS}$. The reliability of OU4 is significantly influenced by destabilizing wave-induced forces during wave crest conditions in S6. Similarly, the maximum overtopping rates are quantified, including both the mean wave overtopping discharge q and the maximum wave overtopping volume V_{max} , for each OU based on 1000 synthetic lifetimes. Consequently, overtopping events are observed exclusively in the main breakwater vertical alignment. Probability Density Functions (PDFs) describing wave overtopping phenomena at these locations are illustrated in Fig. 11. Similarly to the stability analysis mentioned above, there is limited spatial variability in the wave overtopping parameters. However, the probability of failure for the serviceability limit state $P_{f,SLs}$ at each OU is not strictly affected by concurrent events impacting its cross-sections (see Table 4). Furthermore, the overtopping Failure Mode (FM) is slightly more influenced by the mean wave overtopping discharge rate than by the maximum wave

overtopping volume. Lastly, disruptive events related to reliability and serviceability do not occur at the rubble-mound cross-sections.

The analysis of wave agitation Stoppage Modes (SMs) is conducted by evaluating the significant wave height at the specified Area of Operational Interest (AOI) location, which results from the downscaled synthetic time-series within the port. Table 5 presents the operational limit state analysis (OPER) for both wave overtopping and agitation. From the high-resolution assessment, constraint SMs are associated with wave heights exceeding the specified operating thresholds at the transit vessel AOIs. Additionally, non-operability due to wave conditions at berthing AOIs is also relevant, particularly for Operational Units (OUs) 4 to 7. Taking OU7, which is utilized by the container ship terminal, as an example, the wide Probability Density Function (PDF) of annual non-operability hours is primarily influenced by the observed uncertainty in the probabilistic distribution of non-operability conditions in $E1|OU7$ (Fig. 12, left panel). The analysis of wave agitation reveals that wave events leading to non-operability conditions are highly correlated within this Operational Unit (OU). These trends are also observed in the analysis at monthly time-scale (Fig. 12, right panel). In this regard, a notable monthly modulation of non-operability is evident, with the highest values occurring in March.

3.3. Climate-related risk assessment

The final step in the port risk assessment methodology involves connecting structural and operational impacts with the business and management models of the OU. In the context of the business model, the primary objective is to identify the sources of revenue and potential losses within the Operational Unit (OU). This step is crucial for evaluating the economic implications of climate-related impacts and disruptions on the port's operations and financial performance.

In the process of defining the business model, a statistical characterization is conducted to understand the non-climatic drivers that influence the port's trading strategy. This involves identifying a set of socio-economic parameters that are tailored to the specific characteristics of the Operational Unit (OU). The first step in this process is determining the type of cargo handled by the port. This information is essential to connect with the taxable activity associated with the handling of goods within the port's areas and facilities. Tax revenues are often generated based on the volume or value of goods handled, typically through a tax per unit of the product. Furthermore, the long-term assessment of the business performance involves making projections related to factors such as shipment demand, cargo quantities per vessel, and the value of money. These projections help in understanding how the port's financial performance may evolve over time and under different scenarios.

The integrated decision-making process is facilitated by both the structural and operational-based damage models. These models serve different purposes and provide insights into different aspects of the port's performance. The structural-based damage model is event-based, as it relates each repair task to its associated cost. It takes into account different degrees of failure, which may result in varying levels of repair costs. This model is essential for understanding the financial implications of structural failures and repair tasks. Besides, the operational-based damage model is time-averaged over a one-year period. Its primary focus is to represent how the annual non-operability hours (NOP) can lead to a loss of cash flow (Fig. 13). This model considers factors such as the maximum annual non-operability hours without operational consequences ($NOP_{max,Yr}$) and the explanatory function that describes the economic loss mechanism [65,77]. This function can take the form of a linear or sigmoid model for K . It is crucial to evaluate this model annually, as the minimum annual operability hours required to meet expected demand may vary based on factors such as port terminal efficiency and annual traffic growth rates.

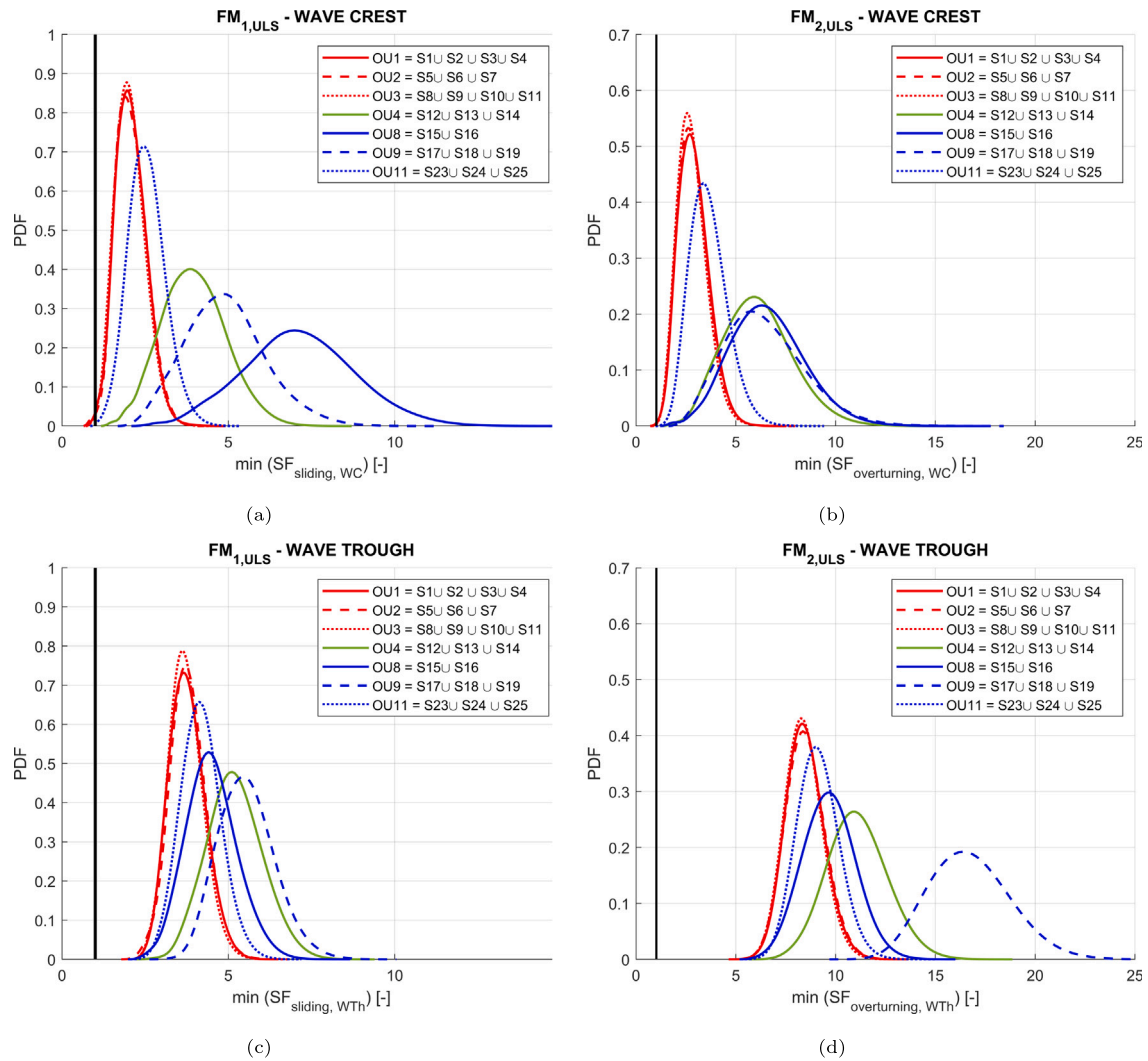


Fig. 10. Probabilistic assessment of the hydraulic performance of OU consisting of vertical breakwaters cross-sections for the sliding (left) and overturning (right) Failure Modes ($FM_{1,ULS}$ and $FM_{2,ULS}$, respectively). Aggregated minimum SF for each synthetic lifetime are displayed. PDFs in upper panels concern Wave Crest (WC) conditions; lower panels to Wave Trough (WTh) conditions. (1000 samples.)

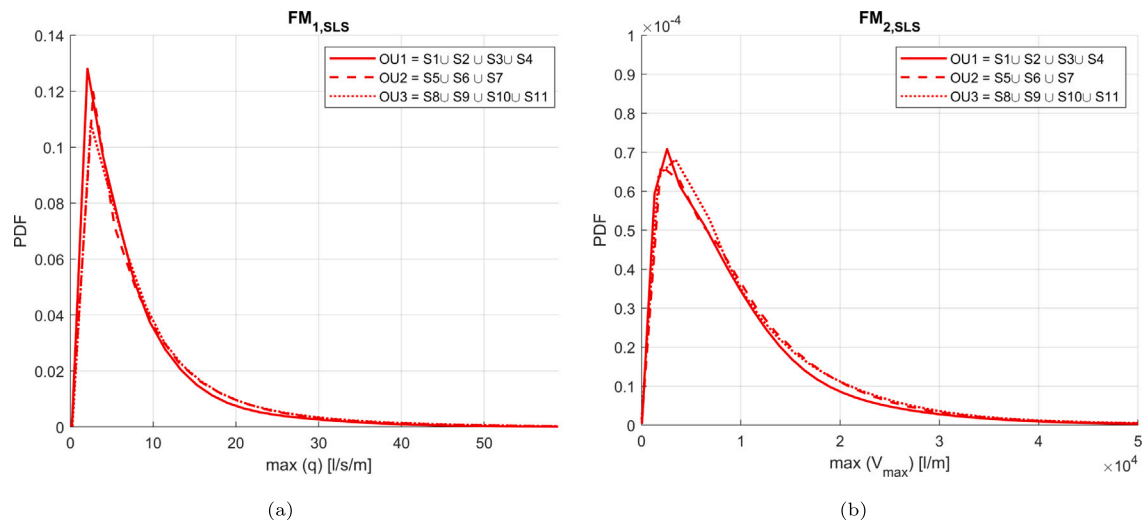


Fig. 11. Probabilistic assessment of the hydraulic performance at OU1, OU2 and OU3 for the wave overtopping failure modes. Aggregated maximum q and V_{max} for each synthetic lifetime are displayed ($FM_{1,SLS}$ and $FM_{2,SLS}$, respectively). PDFs in left panel make reference to the overtopping discharge q parameter; right panel to the maximum wave overtopping volume V_{max} parameter. (1000 samples.)

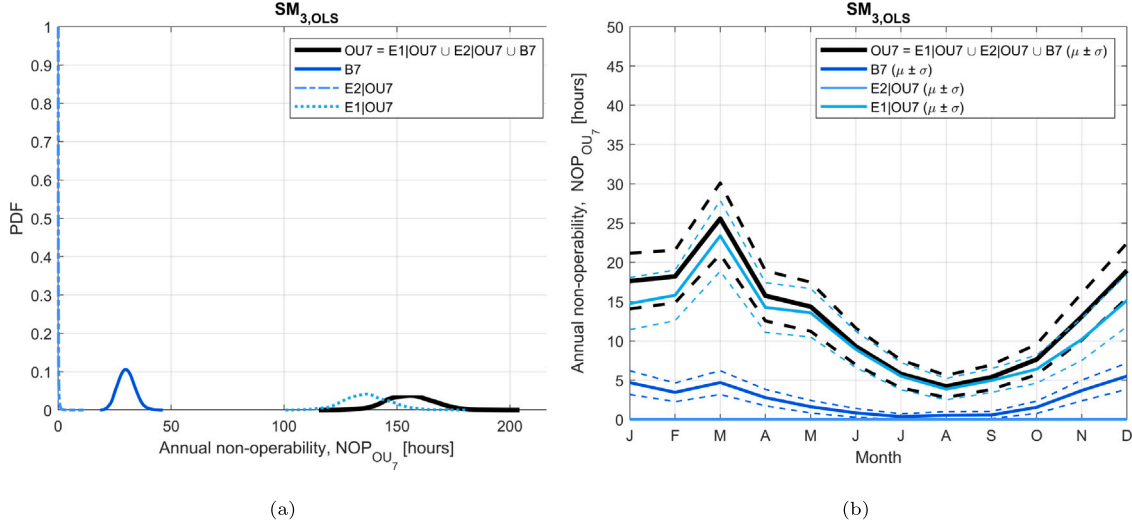


Fig. 12. Probabilistic assessment of the operational performance at OU7 based on the wave agitation (WA) analysis ($SM_{3,OLS}$). PDFs in left panel refer to the statistical distribution of the one-year non-operability wave conditions; right panel to the related intra-annual variability. (1000 samples).

Table 4
Ultimate and Serviceability Limit States (ULS & SLS) verification for the vertical breakwater typologies.

	$FM_{1,ULS}$: Sliding of the caisson		$FM_{2,ULS}$: Overturning of the caisson		$P_{f,ULS}$	$FM_{1,SLS}$ and $FM_{2,SLS}$: Wave overtopping		$P_{f,SLS}$
	$P_{f,WC}$	$P_{f,WTh}$	$P_{f,WC}$	$P_{f,WTh}$		$P_{f,q}$	$P_{f,V_{max}}$	
S1	0.000	0.000	0.000	0.000	0.000	0.023	0.016	0.025
S2	0.001	0.000	0.000	0.000	0.001	0.020	0.016	0.023
S3	0.001	0.000	0.000	0.000	0.001	0.015	0.010	0.018
S4	0.002	0.000	0.000	0.000	0.002	0.029	0.021	0.031
OU1	0.003	0.000	0.000	0.000	0.003	0.065	0.053	0.072
S5	0.001	0.000	0.000	0.000	0.001	0.029	0.016	0.030
S6	0.003	0.000	0.001	0.000	0.003	0.031	0.018	0.032
S7	0.001	0.000	0.000	0.000	0.001	0.034	0.017	0.034
OU2	0.004	0.000	0.001	0.000	0.004	0.070	0.047	0.072
S8	0.000	0.000	0.000	0.000	0.000	0.039	0.026	0.041
S9	0.000	0.000	0.000	0.000	0.000	0.022	0.010	0.023
S10	0.002	0.000	0.001	0.000	0.002	0.010	0.007	0.011
S11	0.000	0.000	0.000	0.000	0.000	0.011	0.009	0.013
OU3	0.002	0.000	0.001	0.000	0.002	0.061	0.045	0.066
S12	0.000	0.000	0.000	0.000	0.000	0.000	0.000	0.000
S13	0.000	0.000	0.000	0.000	0.000	0.000	0.000	0.000
S14	0.000	0.000	0.000	0.000	0.000	0.000	0.000	0.000
OU4	0.000	0.000	0.000	0.000	0.000	0.000	0.000	0.000
S15	0.000	0.000	0.000	0.000	0.000	0.000	0.000	0.000
S16	0.000	0.000	0.000	0.000	0.000	0.000	0.000	0.000
OU8	0.000	0.000	0.000	0.000	0.000	0.000	0.000	0.000
S17	0.000	0.000	0.000	0.000	0.000	0.000	0.000	0.000
S18	0.000	0.000	0.000	0.000	0.000	0.000	0.000	0.000
S19	0.000	0.000	0.000	0.000	0.000	0.000	0.000	0.000
OU9	0.000	0.000	0.000	0.000	0.000	0.000	0.000	0.000
S23	0.001	0.000	0.000	0.000	0.001	0.000	0.000	0.000
S24	0.000	0.000	0.000	0.000	0.000	0.000	0.000	0.000
S25	0.000	0.000	0.000	0.000	0.000	0.000	0.000	0.000
OU11	0.001	0.000	0.000	0.000	0.001	0.000	0.000	0.000

Focusing on the case study, Table 6 summarizes the business model of each port terminal, described by autonomous Operational Units (OUs). Note that OU8, OU9, OU10 and OU11 do not lead to economic benefits. To assess sources of revenue/losses in the OU_j by the year t , annual projections of the terminal traffics $W_{OU_{j,t}}$ as well as the value of goods handled at the port terminal $C_{OU_{j,t}}$ are obtained following

Eqs. (8), and assuming a discount rate r of 3% [78,79].

$$\begin{aligned}
 W_{OU_{j,t}} &= W_{OU_{j,1}} (1 + r_{OU_j})^{t-1} \\
 C_{OU_{j,t}} &= C_{OU_{j,1}} (1 + r)^{t-1} \\
 j &= 1, 2, \dots, 7 \quad ; \quad t = 1, 2, \dots, 50
 \end{aligned} \tag{8}$$

Table 5
Operability Limit State verification (OLS) for the vertical breakwater typologies.

	$SM_{1,OLS}$ and $SM_{2,OLS}$: Wave overtopping		$SM_{3,OLS}$: Wave agitation	$SM_{1,OLS}$
	$OPER_q$	$OPER_{V_{max}}$	$OPER_{WA}$	
S1	0.9998	0.9999	–	0.9998
S2	0.9998	0.9999	–	0.9998
S3	0.9999	0.9999	–	0.9999
S4	0.9998	0.9998	–	0.9998
B1	–	–	0.9998	0.9998
E1 OU1	–	–	0.9805	0.9805
E2 OU1	–	–	0.9999	0.9999
OU1	0.9997	0.9998	0.9805	0.9805
S5	0.9998	0.9998	–	0.9998
S6	0.9998	0.9999	–	0.9998
S7	0.9998	0.9998	–	0.9998
B2	–	–	0.9997	0.9997
E1 OU2	–	–	0.9805	0.9805
E2 OU2	–	–	0.9999	0.9999
OU2	0.9997	0.9998	0.9805	0.9805
S8	0.9998	0.9998	–	0.9998
S9	0.9998	0.9999	–	0.9998
S10	0.9998	0.9999	–	0.9998
S11	0.9999	0.9999	–	0.9999
B3	–	–	0.9997	0.9997
E1 OU3	–	–	0.9805	0.9805
E2 OU3	–	–	0.9999	0.9999
OU3	0.9997	0.9998	0.9805	0.9805
S12	1.0000	1.0000	–	1.0000
S13	1.0000	1.0000	–	1.0000
S14	1.0000	1.0000	–	1.0000
B4	–	–	0.9949	0.9949
E1 OU4	–	–	0.9805	0.9805
E2 OU4	–	–	0.9999	0.9999
OU4	1.0000	1.0000	0.9805	0.9805
B5	–	–	0.9932	0.9932
E1 OU5	–	–	0.9805	0.9805
E2 OU5	–	–	0.9999	0.9999
OU5	–	–	0.9804	0.9804
B6	–	–	0.9960	0.9960
E1 OU6	–	–	0.9805	0.9805
E2 OU6	–	–	0.9999	0.9999
OU6	–	–	0.9800	0.9800
B7	–	–	0.9952	0.9952
E1 OU7	–	–	0.9805	0.9805
E2 OU7	–	–	0.9999	0.9999
OU7	–	–	0.9779	0.9779
S15	1.0000	1.0000	–	1.0000
S16	1.0000	1.0000	–	1.0000
OU8	1.0000	1.0000	–	1.0000
S17	1.0000	1.0000	–	1.0000
S18	1.0000	1.0000	–	1.0000
S19	1.0000	1.0000	–	1.0000
OU9	1.0000	1.0000	–	1.0000
S20	1.0000	1.0000	–	1.0000
S21	1.0000	1.0000	–	1.0000
S22	1.0000	1.0000	–	1.0000
OU10	1.0000	1.0000	–	1.0000
S23	1.0000	1.0000	–	1.0000
S24	1.0000	1.0000	–	1.0000
S25	1.0000	1.0000	–	1.0000
OU11	1.0000	1.0000	–	1.0000

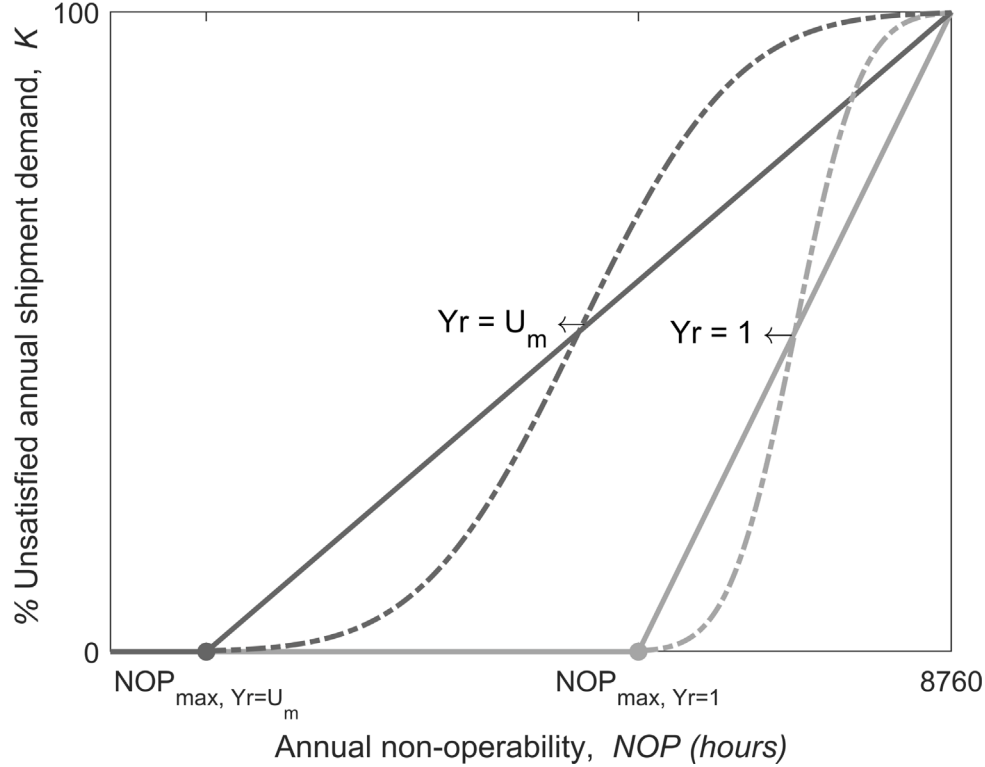
Structural-based damage models are defined for the coastal structures and port equipment belonging to each OU. L events triggering the failure of any S coastal defense and taking place in year t , are evaluated assuming a cost of repair V_l proportional to its project initial cost

$I_{0,S}$. It is also assumed for estimating expected consequences derived from P disruptive events inducing a serviceability failure in PE . Event-based damage functions (α ranging from 0 to 1) are characterized for assessing failure related consequences as explained in [80]. In this case,

Table 6

Detailed business model characterization of the existing port terminals according to the OU division.

	Type of cargo	Incoming & outgoing goods in the 1st year, $W_{OU,j,1}$	Growth rate, $r_{OU,j}$	Occupancy rate, $\Phi_{OU,j}$	Port equipment performance, $\eta_{OU,j}$	Value (tax) of goods in the 1st year, $C_{OU,j,1}$
OU1 OU2 OU3	Liquid gas	145,000 tons	2.0%	11.0%	400 tons/h	4 €/ton
OU4	Ro-ro	19,750 units	1.6%	11.0%	45 units/h	50 €/unit
OU5	Ro-pax	265,000 pax	1.0%	11.0%	450 pax/h	7 €/pax
OU6	Containers	50,000 TEUs	2.3%	14.0%	125 TEUs/h	25 €/TEU
OU7	Containers	44,500 TEUs	1.7%	14.0%	83.5 TEUs/h	25 €/TEU

**Fig. 13.** Operational-based damage models relating the annual non-operability with the unsatisfied annual demand. In the scenario of demand growth, the expected economic losses increase over time (From year $Yr = 1$ to the end of its lifetime $Yr = U_m$).

it is assumed that the cost of repair (V_l) is equal to twice ($\alpha_l = 2$) the initial project cost (I_{0_S}). Regarding V_p , it is assumed to be equal to half ($\alpha_p = 0.5$) the initial investment cost ($I_{0_{PE}}$). Both damage models are shown in Eq. (9).

$$\begin{aligned}
 V_l &= \alpha_l I_{0_S} (1+r)^{t-1} \\
 V_p &= \alpha_p I_{0_{PE}} (1+r)^{t-1} \\
 l &= 1, 2, \dots, L \quad ; \quad p = 1, 2, \dots, P \quad ; \quad S = 1, 2, \dots, 11 \quad ; \quad t = 1, 2, \dots, 50
 \end{aligned}
 \quad (9)$$

Operational-based damage models relates annual non-operability hours due to wave-related hazards with the cash flow losses in the analyzed Operational Unit (OU) as a result of port activity stoppages. Stoppage Modes (SMs) trigger an operational impact with the same length of time as wave action. Aggregating annual non-operability hours $NOP_{OU,j,t}$, unsatisfied annual shipment demand $K_{OU,j,t}$ is evaluated. If it exceeds the maximum annual non-operability hours allowed to service the goods to be handled during the year, $NOP_{max,OU,j,t}$, operational related consequences $O_{OU,j,t}$ are calculated in proportion to the intensity of the previously quantified non-operability (linear model, Eq. (10)). The tipping point $NOP_{max,OU,j,t}$ [65,77], which separates the

fully-operability region from the partially/fully non-operability region, is evaluated as a function of the port terminal traffic $W_{OU,j,t}$, the occupancy rate at the berthing area $\Phi_{OU,j}$ and the port equipment performance for loading and unloading goods $\eta_{OU,j}$ for each Operational Unit (OU) every year (Eq. (11)). As can be noted, it decreases as the expected traffic grows.

$$O_{OU,j,t} = \begin{cases} = 0 & \text{if } NOP_{OU,j,t} \leq NOP_{max,OU,j,t} \\ = \left[\frac{K_{OU,j,t}}{100} \right] W_{OU,j,t} C_{OU,j,t} & \text{otherwise} \end{cases}
 \quad j = 1, 2, \dots, 7; t = 1, 2, \dots, 50
 \quad (10)$$

$$NOP_{max,OU,j,t} = 8760 - \frac{W_{OU,j,t}}{\Phi_{OU,j} \eta_{OU,j}}
 \quad j = 1, 2, \dots, 7 \quad ; \quad t = 1, 2, \dots, 50
 \quad (11)$$

This systematic approach allows for a realistic estimation of how climate drivers interact with socio-economic drivers within the Operational Unit (OU) environment of the port [78,81]. By following this process OU by OU, the climate-related risk to the port can be assessed.

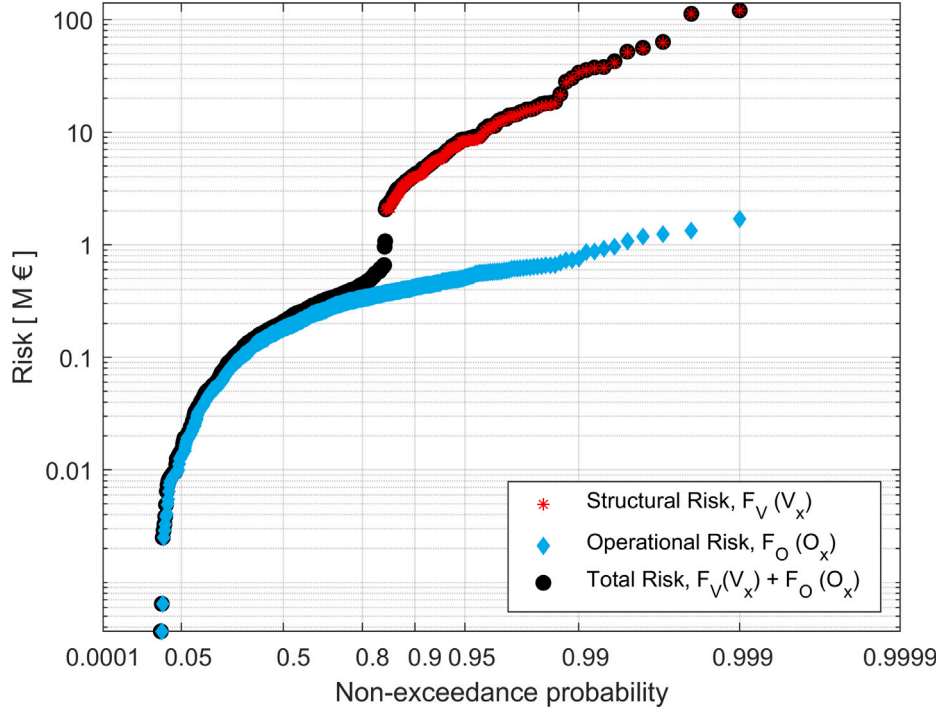


Fig. 14. Maximal distributions of cumulative losses due to damage to coastal structures and port equipment (Structural risk) and port operations (Operational risk). Total risk refers to the sum of structural and operational risks. (1000 samples).

This assessment can be probabilistic in nature, taking into account both the structural and operational components. Additionally, profitability measures such as the internal rate of return (IRR), the net present value (NPV), and the payback period can be quantified [79,82]. These financial metrics are commonly used in decision-making processes and help identify Operational Units (OUs) with a higher probability of adverse consequences and their triggering causes. This information is crucial for discerning critical OUs and port components that require effective action and investment planning.

Climate-related risks are computed according to the N_T 1000 fifty-year long synthetic lifetimes. Structural risk ($F_V(V_x)$) is obtained as a result of the sum of the individual costs for ULS- and SLS-impact events. The sum of the annual operational consequences in each of the Operational Unit (OU) is used to estimate operational risk ($F_O(O_x)$) in the port environment. As observed in Fig. 14, operational risk is predominant for approximately 85% of the simulated lifetimes. Structural risk appears to be dominant in the remaining synthetic cases. In this regard, it is important to emphasize the occurrence of these low probability high-impact scenarios (structural risk can be 100 times higher than operational risk with an occurrence probability of 0.1%). Nevertheless, total risk ranges from 0.015 to 8.639 million euros with 90% confidence interval. Such analysis determines that climate-related risk lower than 10 million euros is expected at the end of the 50-year lifetime with a 95% probability. Likewise, profitability of port project investments can be probabilistically assessed. In this work, its proposed applying the Internal Return Rate IRR (Eq. (12)) as a dimensionless index [79,82]. Assuming the entire port investment I_0 takes place in the first year, expected cash flows can be assessed. From the Monte Carlo simulations, an IRR varying from 4.98 to 5.04% can be obtained with a 90% confidence interval (Fig. 15). Besides, the return of the investment is highly influenced by events triggering a structural failure. In any case, the project is accepted since the internal return rate is greater

than the cost of capital (3%) for all the synthetic lifetimes.

$$IRR [\%] : -I_0 - \sum_{l=1}^L \frac{V_l}{\left(1 + \frac{IRR}{100}\right)^{l-1}} - \sum_{p=1}^P \frac{V_p}{\left(1 + \frac{IRR}{100}\right)^{p-1}} + \sum_{j=1}^7 \sum_{i=1}^{U_m=50} \frac{\left(1 - \frac{K_{OU_{j,i}}}{100}\right) W_{OU_{j,i}} C_{OU_{j,i}}}{\left(1 + \frac{IRR}{100}\right)^{i-1}} = 0 \quad (12)$$

4. Discussion and conclusions

This research addresses the critical impact of climate dynamics on coastal and port infrastructures. The primary objective of this innovative framework is to comprehensively evaluate climate-induced consequences, thereby facilitating informed decision-making processes in the domains of coastal and port infrastructure design, management, and adaptation. It achieves this by integrating the well-established Spanish Recommendations for Maritime Works (ROM) with the structured risk assessment approach advocated by the Intergovernmental Panel on Climate Change (IPCC).

This unified framework incorporates climate science, engineering principles, and risk assessment methodologies to provide a holistic view of climate-related impacts and risks. It recognizes the site-specific hazards, exposure and vulnerabilities of coastal and port infrastructures, emphasizing the importance of performing high-resolution analysis. Furthermore, it addresses the challenge of decision-making under deep uncertainty, particularly in the context of climate change analysis. The cascade of uncertainty, from global climate modeling to site-specific assessments, underscores the need for robust management of uncertainty throughout the process. It has been achieved applying [30] statistical method to infer low-probability-high-impact events and a probabilistic framework based on Monte Carlo technique to assess its reliability, functionality and operability.

The challenge of conducting a high-resolution analysis of climate-related impacts and risks at the port scale is a complex endeavor that

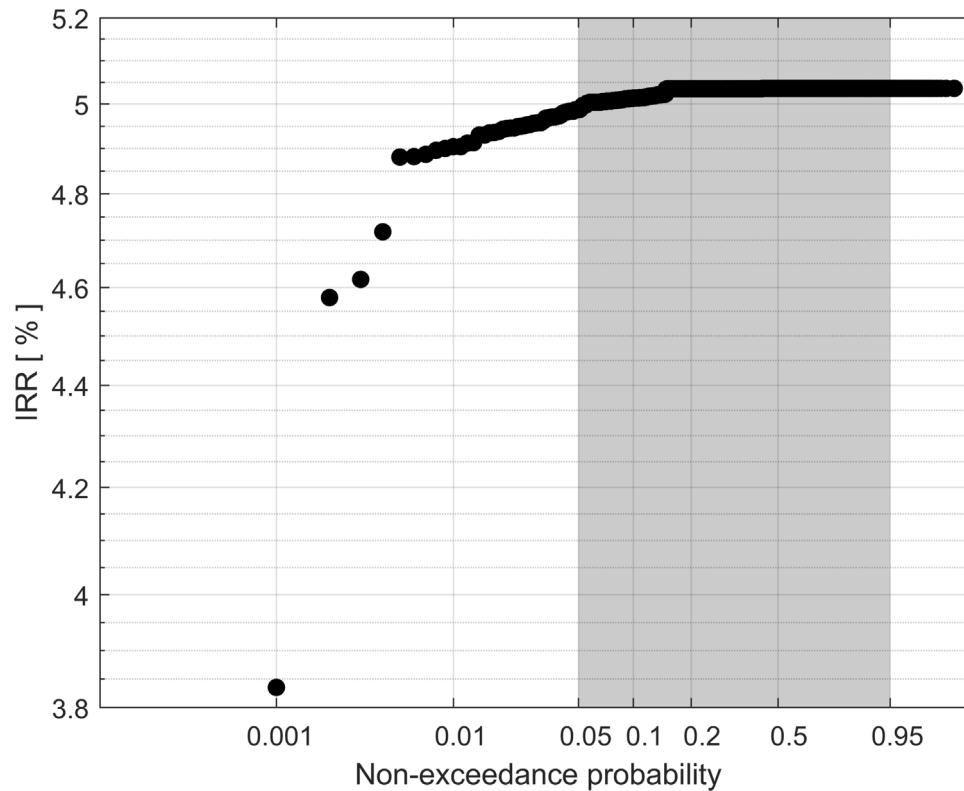


Fig. 15. Minimal distribution of profitability expressed as a percentage of the Internal Return Rate (IRR). The shaded area represents the 90% confidence interval for the 1000 samples.

requires detailed consideration of hazards, exposure, and vulnerability factors. Hazards, particularly wave dynamics, exhibit significant variability both along breakwater alignments and within harbor basins, necessitating a precise assessment of their effects on coastal structures and operational areas. Exposure assessment must encompass detailed descriptions of coastal structure features and the spatial arrangement of port equipment, linking this information with vulnerability assessments to establish tolerable states for exposed assets. To address the variability among exposed assets and port operations, a novel concept of Operational Units (OUs) has been introduced. OUs represent homogeneous and independent port entities handling specific cargo typologies, integrating both technical and governance aspects. This concept enables a comprehensive risk-based analysis that considers spatial, temporal, and profit variability at the port scale. The framework is developed and implemented at the OU scale, allowing for the aggregation of risks associated with individual OUs to calculate the overall risk for the entire port. This holistic approach provides a robust foundation for assessing climate-related impacts and risks in a high-resolution manner within the complex port environment.

Focusing on the case study, this research has delved deep into the pivotal role that ports play in the global economy, particularly highlighting their significance as nodal points in the logistics system. The global trade statistics presented underscore the magnitude of their contribution, with maritime transport serving as the lifeblood of international trade. The strategic importance of ports has been emphasized, driven by the economies of scale associated with maritime transport and the imperative to accommodate larger vessels necessitating robust coastal infrastructure. In particular, the new framework for assessing climate-related impacts and risks has been extended to encompass ports of international importance. These ports are economic linchpins, essential for the economic activities of nations. The case of Spain's state-owned ports exemplifies their strategic value and diverse functions, from handling various cargo types to large-scale infrastructure investments and revenue generation. In this regard, the concept of

the Operational Unit (OU) has emerged as a critical tool for precise evaluation of revenue sources and potential economic losses, a crucial aspect in assessing the impact of climate-related events.

The description of exposure necessitates a comprehensive definition encompassing all aspects of port facilities and operations susceptible to not meeting reliability, functionality, and operational requirements due to failure modes and/or stoppages. This entails a precise characterization of their attributes to accurately quantify the disruptive mechanisms involved. In the context of vulnerability characterization, this study introduces a novel probabilistic approach to assess the sensitivity of exposed elements to disruptive events, aimed at addressing the uncertainty surrounding threshold states. As demonstrated through a case study, conducting a thorough analysis of vulnerability is imperative for achieving a realistic statistical characterization. Furthermore, continuous monitoring of structural performance and operations by port users throughout its lifespan plays a crucial role in reducing uncertainties associated with vulnerability estimates. This proactive engagement is vital for the refinement and improvement of impact model assessments. For hazard, Lucio et al. [30] has been applied to comprehensively simulate synthetic time series of compound events, aiming to assess the safety, functionality, and operability design requirements for coastal structures under conditions of uncertainty.

The climate-related impact and risk assessment methodology has been introduced as effective tool to aid decision-making processes by pinpointing critical areas within the port system. The approach outlined in this research enhances the knowledge of port managers by identifying critical areas within the port system, thereby facilitating the planning of adaptation strategies to ensure its technical viability. Additionally, the inclusion of a business model and management policy allows for the translation of technical-based findings into economic consequences. This provides insights into how climatic hazards interact with non-climatic drivers, such as projections of shipment demand, cargo volumes per vessel, and the value of goods. In the case study, a deterministic non-stationary socio-economic scenario is considered,

assuming independent Operational Units (OUs), meaning that the activities at one OU do not influence others. This approach results in probabilistic estimates of structural and operational risks, which can be attributed to investments in port infrastructure and potential losses in taxable activities, respectively. Overall, this methodology provides valuable insights into the economic viability of the port, in addition to addressing technical requirements and climate-related challenges. To summarize the main conclusions drawn from the application of the new port-oriented impact assessment methodology, the research questions posed in Introduction can be answered as follows: The coastal structure is currently safe, functional and operational. High margin levels are inferred for the Ultimate Limit State (ULS) and Operational Limit State (OLS), being lower for the Serviceability Limit State (SLS). Failure modes triggered by wave overtopping are prone to be influenced by wave dynamics. Despite not exceeding tolerable risks levels set in the design phase, it can be relevant from OU1 to OU3. Port facilities located on the top of the crown wall and maneuvering and sailing areas carried out in the shelter are prone to be critical due to wave overtopping.

Finally, future research should prioritize the development of methodological frameworks for implementing cost-effective strategies to address climate change within taking this port-oriented risk framework as a reference. These adaptation strategies should include plans for human interventions that are both temporally and spatially optimized to ensure the technical requirements and economic viability of port infrastructure. Specifically, it is recommended to adopt Dynamic Adaptive Policy Pathways (DAPPs), as proposed by Haasnoot et al. [83]. DAPPs offer a structured approach that combines precise uncertainty management (as discussed in [84]) with a flexible action plan that can adapt to changing circumstances. By combining a probabilistic projection of non-climatic variables, such as the stochastic evolution over time of goods handled at a specific Operational Unit (OU), with climatic factors, a comprehensive probabilistic assessment [80] of future risks due to climate change can be achieved. DAPPs are designed as roadmaps, outlining decision points where (1) decisions are made (prior to reaching the maximum tolerable risk level), (2) actions are implemented (when the risk level equals or exceeds the maximum tolerable risk), and (3) a predefined set of possible strategies is executed.

List of acronyms

AOI Area of Operational interest.

AT Astronomical Tide, in meters.

Dir Mean wave direction, in degrees.

DOW Downscaled Ocean Waves database.

FM Failure Mode.

IPCC Intergovernmental Panel on Climate Change, whose mission is providing governments and stakeholders scientific information that they can use to develop climate policies.

IRR Internal Return Rate.

OLS Operational Limit State. Stoppage modes triggering a shutdown of port operations belong to OLS.

OU Operational Unit.

PDF Probability Density Function.

ROM Spanish Recommendations for Maritime Works.

SF Safety Factor.

SEF Semi-Empirical Formula.

SLS Serviceability Limit State. Failure modes triggering a damage to the coastal infrastructure without structural consequences belong to SLS.

SM Stoppage Mode.

SS Storm Surge, in meters.

SWL Still Water Level, defined as the sea-level without considering wave-induced components ($SWL = AT + SS$), in meters.

ULS Ultimate Limit State. Failure modes triggering a damage to the coastal infrastructure with structural consequences belong to ULS.

Wc Wave pressure under wave crest conditions.

WTh Wave pressure under wave trough conditions.

List of symbols

B Berthing area of a certain Operational Unit.

C_{OU} Value of goods handled in a certain Operational Unit.

CV Coefficient of variation of a certain parameter, computed as the ratio of the standard deviation (σ) to the mean (μ), $CV = \sigma \div \mu$.

E Manoeuvring area of a certain Operational Unit.

F(Ψ) Fragility curve.

f_{threshold}(Ψ) Probability density function of a Ψ variable. It means the same that PDF.

g(R,S) Impact function.

H_s Significant wave height, defined as the average height of the highest one-third of the waves belonging to the sea-state, in meters.

I₀ Port project investment.

K Percentage of unsatisfied annual shipment demand.

K_r Reflection coefficient.

N_f Synthetic realizations (lifetimes) with failure.

N_{od} Damage parameter. It refers to the relative eroded area in rock armor layers.

N_T Synthetic realizations (lifetimes).

NOP Annual non-operable hours.

NOP_{max} Maximum annual non-operable hours allowed to service goods to be handled during a certain year.

O(t) Operational risk, in euros.

OPER Minimum annual port operability quantified for the OLS.

PE Port equipment of a certain Operational Unit.

P_{f,SLS} Maximum joint probability of failure quantified for the SLS

P_{f,ULS} Maximum joint probability of failure quantified for the ULS.

q Mean wave overtopping discharge in a sea-state, in liters per seconds per meter width.

r Discount rate.

S Coastal structure characterized by its cross-section of a certain Operational Unit.

T_m Mean wave period of the sea-state, in seconds.

T_p Peak wave period of the sea-state, defined as the inverse of the frequency with the highest spectral energy density, in seconds.

U_m Minimum useful life of the coastal structure, in years.

V(t) Structural risk, in euros.

V_{max} Maximum wave overtopping volume in a sea-state, in liters per meter width.

W_{OU} Goods handled in a certain Operational Unit.

α_l Event-based damage function for the assessment of climate-related consequences on coastal structures.

α_p Event-based damage function for the assessment of climate-related consequences on port equipment.

Ψ Governing parameter which describes a certain failure/stoppage mode.

Ψ_{crit} Critical value of a certain governing parameter for each synthetic lifetime within Monte Carlo procedure.

$\Psi_{threshold}$ Threshold value of a certain governing parameter splitting failure and safe regions.

Φ_{OU} Occupancy rate of a certain Operational Unit.

η Port Equipment performance.

CRediT authorship contribution statement

D. Lucio: Writing – review & editing, Writing – original draft, Software, Methodology, Investigation, Data curation, Conceptualization. **J.L. Lara:** Validation, Supervision, Project administration, Investigation, Funding acquisition, Conceptualization. **A. Tomás:** Writing – review & editing, Validation, Project administration, Funding acquisition, Formal analysis, Conceptualization. **I.J. Losada:** Writing – review & editing, Methodology, Investigation, Conceptualization.

Declaration of competing interest

The authors declare that they have no known competing financial interests or personal relationships that could have appeared to influence the work reported in this paper.

Data availability

Data will be made available on request.

Acknowledgments

D. Lucio is indebted to the Spanish Ministry of Science, Innovation and Universities for the funding provided in the FPI studentship (PRE2018-086142). This work has been also partially funded under the RETOS program (BIA2017-87213-R) and the State R&D Program Oriented to the Challenges of the Society (PID2020-118285RB-I00) of the Spanish Ministry of Science, Innovation and Universities.

Appendix A. Supplementary data

Supplementary material related to this article can be found online at <https://doi.org/10.1016/j.res.2024.110333>.

References

- [1] Baird A.J. Public goods and the public financing of major European seaports. *Marit Policy Manag* 2004;31(4):375–91.
- [2] UNCTAD. Review of maritime transport 2018. In: United Nations Conference on Trade and Development. 2018, p. 115.
- [3] Verschuur J, Koks E, Hall J. Systemic risks from climate-related disruptions at ports. *Nat Clim Change* 2023;13:804–6.
- [4] ROM00-01. Spanish recommendations for maritime structures. In: General procedure and requirements design of harbor and maritime structures. Part I. Puertos del Estado: Spanish Ministry of Public Works and Transport; 2001, p. 220.
- [5] ROM:10-09. Spanish recommendations for the project design and construction of breakwaters. Part I: Calculation and project factors. Puertos del Estado: Climate Agents; 2009, URL <http://www.puertos.es/es-es/ROM/Paginas/ROM-widispe.aspx>.
- [6] ROM:11-18. Spanish recommendations for maritime works: Recommendations for breakwater construction projects. Puertos del Estado; 2018, URL <http://www.puertos.es/es-es/ROM/Paginas/ROM-widispe.aspx>.
- [7] Notteboom T. Chapter 19 concession agreements as port governance tools. *Res Transp Econ* 2006;17:437–55, Devolution, Port Governance and Port Performance.
- [8] Notteboom T, Parola F, Satta G, Penco L. Disclosure as a tool in stakeholder relations management: a longitudinal study on the port of Rotterdam. *Int J Logist Res Appl* 2015;18(3):228–50. <http://dx.doi.org/10.1080/13675567.2015.1027149>.
- [9] Meda-Bartual A, Molinos-Senante M, Sala-Garrido R. Productivity change of the Spanish port system: impact of the economic crisis. *Marit Policy Manag* 2016;43(6):683–705. <http://dx.doi.org/10.1080/03088839.2016.1182653>.
- [10] Núñez-Sánchez R, Coto-Millán P. The impact of public reforms on the productivity of Spanish ports: A parametric distance function approach. *Transp Policy* 2012;24:99–108. <http://dx.doi.org/10.1016/j.tranpol.2012.07.011>.
- [11] Alises A, Molina R, Gómez R, Pery P, Castillo C. Overtopping hazards to port activities: Application of a new methodology to risk management (PORT risk MAnagement tool). *Reliab Eng Syst Saf* 2014;123:8–20. <http://dx.doi.org/10.1016/j.res.2013.09.005>.
- [12] Gómez R, Molina R, Castillo C, Rodríguez I, López JD. Conceptos y herramientas probabilísticas para el cálculo del riesgo en el ámbito portuario. *Puertos del Estado*; 2019, p. 291.
- [13] Sierra J, Genius A, Lionello P, Mestres M, Mosso C, Marzo L. Modelling the impact of climate change on harbour operability: The Barcelona port case study. *Ocean Eng* 2017;141:64–78. <http://dx.doi.org/10.1016/j.oceaneng.2017.06.002>.
- [14] Campos Á, García-Valdecasas JM, Molina R, Castillo C, Álvarez-Fanjul E, Staneva J. Addressing long-term operational risk management in port docks under climate change scenarios—A Spanish case study. *Water* 2019;11(10). <http://dx.doi.org/10.3390/w11102153>.
- [15] Camus P, Tomás A, Díaz-Hernandez G, Rodríguez B, Izaguirre C, Losada I. Probabilistic assessment of port operation downtimes under climate change. *Coast Eng* 2019;147:12–24. <http://dx.doi.org/10.1016/j.coastaleng.2019.01.007>.
- [16] Casas-Prat M, Sierra J. Trend analysis of wave storminess: Wave direction and its impact on harbour agitation. *Nat Hazards Earth Syst Sci* 2010;10(11):2327–40. <http://dx.doi.org/10.5194/nhess-10-2327-2010>.
- [17] Sierra J, Casanovas I, Mosso C, Mestres M, Sánchez-Arcilla A. Vulnerability of catalan (NW mediterranean) ports to wave overtopping due to different scenarios of sea level rise. *Reg Environ Change* 2016;16(5):1457–68.
- [18] Camus P, Losada IJ, Izaguirre C, Espejo A, Menéndez M, Pérez J. Statistical wave climate projections for coastal impact assessments. *Earth's Future* 2017;5:918–33.
- [19] Sierra JP, Casas-Prat M, Virgili M, Mosso C, Sánchez-Arcilla A. Impacts on wave-driven harbour agitation due to climate change in catalan ports. *Nat Hazards Earth Syst Sci* 2015;15(8):1695–709. <http://dx.doi.org/10.5194/nhess-15-1695-2015>.
- [20] Izaguirre C, Losada I, Camus P, Vigh J, Stenek V. Climate change risk to global port operations. *Nature Clim Change* 2021;11(1):14–20. <http://dx.doi.org/10.1038/s41558-020-00937-z>.
- [21] Burcharth HF, Lykke Andersen T, Lara JL. Upgrade of coastal defence structures against increased loadings caused by climate change: A first methodological approach. *Coast Eng* 2014;87:112–21. <http://dx.doi.org/10.1016/j.coastaleng.2013.12.006>.
- [22] Galiatsatou P, Makris C, Prinos P. Optimized reliability based upgrading of rubble mound breakwaters in a changing climate. *J Mar Sci Eng* 2018;6(3):92.
- [23] Suh K-D, Kim S-W, Mori N, Mase H. Effect of climate change on performance-based design of caisson breakwaters. *J Waterw Port Coast Ocean Eng* 2012;138(3):215–25.

- [24] Lee C-E, Kim S-W, Park D-H, Suh K-D. Target reliability of caisson sliding of vertical breakwater based on safety factors. *Coast Eng* 2012;60:167–73. <http://dx.doi.org/10.1016/j.coastaleng.2011.09.005>.
- [25] Castillo C, Mínguez R, Castillo E, Losada M. An optimal engineering design method with failure rate constraints and sensitivity analysis. Application to composite breakwaters. *Coast Eng* 2006;53(1):1–25. <http://dx.doi.org/10.1016/j.coastaleng.2005.09.016>.
- [26] Mínguez R, Castillo E, Castillo C, Losada MA. Optimal cost design with sensitivity analysis using decomposition techniques. Application to composite breakwaters. *Struct Saf* 2006;28(4):321–40. <http://dx.doi.org/10.1016/J.STRUSAFE.2005.08.005>.
- [27] Nadal-Caraballo N, Melby J, Gonzalez V. Statistical analysis of historical extreme water levels for the U.S. North Atlantic coast using Monte Carlo life-cycle simulation. *J Coast Res* 2016;32(1):35–45. <http://dx.doi.org/10.2112/JCOASTRES-D-15-00031.1>.
- [28] Wahl T, Muddersbach C, Jensen J. Assessing the hydrodynamic boundary conditions for risk analyses in coastal areas: A multivariate statistical approach based on copula functions. *Nat Hazards Earth Syst Sci* 2012;12(2):495–510. <http://dx.doi.org/10.5194/nhess-12-495-2012>.
- [29] Solari S, Losada MA. Non-stationary wave height climate modeling and simulation. *J Geophys Res: Oceans* 2011;116(C9). <http://dx.doi.org/10.1029/2011JC007101>.
- [30] Lucio D, Tomás A, Lara J, Camus P, Losada I. Stochastic modeling of long-term wave climate based on weather patterns for coastal structures applications. *Coast Eng* 2020;161:103771. <http://dx.doi.org/10.1016/j.coastaleng.2020.103771>.
- [31] Lucio D, Lara J, Tomás A, Losada I. Projecting compound wave and sea-level events at a coastal structure site under climate change. *Coast Eng* 2024;189:104490. <http://dx.doi.org/10.1016/j.coastaleng.2024.104490>.
- [32] Cao X, Lam JSL. Simulation-based catastrophe-induced port loss estimation. *Reliab Eng Syst Saf* 2018;175:1–12. <http://dx.doi.org/10.1016/j.res.2018.02.008>.
- [33] Almutairi A, Collier ZA, Hendrickson D, Palma-Oliveira JM, Polmateer TL, Lambert JH. Stakeholder mapping and disruption scenarios with application to resilience of a container port. *Reliab Eng Syst Saf* 2019;182:219–32. <http://dx.doi.org/10.1016/j.res.2018.10.010>.
- [34] Wang N, Wu M, Yuen KF. Assessment of port resilience using Bayesian network: A study of strategies to enhance readiness and response capacities. *Reliab Eng Syst Saf* 2023;237:109394. <http://dx.doi.org/10.1016/j.res.2023.109394>.
- [35] IPCC. Summary for policymakers. In: *Climate change 2022: Impacts, adaptation, and vulnerability. Impacts, adaptation and vulnerability. Contribution of working group II to the sixth assessment report of the IPCC*. Cambridge, United Kingdom and New York, NY, USA: Cambridge University Press; 2022, p. 3–33.
- [36] Wilby RL, Dessai S. Robust adaptation to climate change. *Weather* 2010;65(7):180–5.
- [37] PIANC. Report N° 196-2016. criteria for the selection of breakwater types and their related optimum safety levels. In: *The World Association for Waterborne Transport Infrastructure*. 2016.
- [38] Burcharth HF, Sorensen JD, Kim S-W. Handbook of coastal and ocean engineering. 2018, p. 313–71. http://dx.doi.org/10.1142/9789813204027_0013, URL https://www.worldscientific.com/doi/abs/10.1142/9789813204027_0013, [Chapter 13: Optimum Safety Levels of Breakwaters].
- [39] Zhou Y, Li X, Yuen KF. Holistic risk assessment of container shipping service based on Bayesian network modelling. *Reliab Eng Syst Saf* 2022;220:108305. <http://dx.doi.org/10.1016/j.res.2021.108305>.
- [40] Burcharth HF. Reliability evaluation and probabilistic design of coastal structures. In: *International seminar on hydro-technical engineering for future development of ports and harbors*. Unyusho Kowan Gijutsu Kenkyujo; 1993.
- [41] Baker JW. Efficient analytical fragility function fitting using dynamic structural analysis. *Earthq Spectra* 2015;31(1):579–99. <http://dx.doi.org/10.1193/021113EQS025M>.
- [42] Zentner I. A general framework for the estimation of analytical fragility functions based on multivariate probability distributions. *Struct Saf* 2017;64:54–61. <http://dx.doi.org/10.1016/j.strusafe.2016.09.003>.
- [43] Castillo C, Castillo E, Fernández-Canteli A, Molina R, Gómez R. Stochastic model for damage accumulation in rubble-mound breakwaters based on compatibility conditions and the central limit theorem. *J Waterw Port Coast Ocean Eng* 2012;138(6):451–63. [http://dx.doi.org/10.1061/\(ASCE\)WW.1943-5460.0000146](http://dx.doi.org/10.1061/(ASCE)WW.1943-5460.0000146).
- [44] Lira-Loarca A, Cobos M, Losada MÁ, Baquerizo A. Storm characterization and simulation for damage evolution models of maritime structures. *Coast Eng* 2019;103620. <http://dx.doi.org/10.1016/j.coastaleng.2019.103620>.
- [45] Zscheischler J, Westra S, Van Den Hurk B, Seneviratne S, Ward P, Pitman A, Aghakouchak A, Bresch D, Leonard M, Wahl T, Zhang X. Future climate risk from compound events. *Nature Clim Change* 2018;8(6):469–77. <http://dx.doi.org/10.1038/s41558-018-0156-3>.
- [46] Zscheischler J, Martius O, Westra S. A typology of compound weather and climate events. *Nat Rev Earth Environ* 2020;1:333–47.
- [47] Salvadori G, Michele CD, Kotegoda NT, Rosso R. Extreme value analysis via copulas. In: *Extremes in nature: an approach using copulas*. Dordrecht: Springer Netherlands; 2007, p. 191–208. http://dx.doi.org/10.1007/1-4020-4415-1_5.
- [48] Michele CD, Salvadori G, Passoni G, Vezzoli R. A multivariate model of sea storms using copulas. *Coast Eng* 2007;54(10):734–51. <http://dx.doi.org/10.1016/j.coastaleng.2007.05.007>.
- [49] Jäger W, Nápoles O. A vine-copula model for time series of significant wave heights and mean zero-crossing periods in the north sea. *ASCE-ASME J Risk Uncertain Eng Syst A Civ Eng* 2017;3:04017014.
- [50] Lin-Ye J, García-León M, Gràcia V, Ortego M, Lionello P, Sánchez-Arcilla A. Multivariate statistical modelling of future marine storms. *Appl Ocean Res* 2017;65:192–205. <http://dx.doi.org/10.1016/j.apor.2017.04.009>.
- [51] Jäger W, Nagler T, Czado C, McCall R. A statistical simulation method for joint time series of non-stationary hourly wave parameters. *Coast Eng* 2019;146:14–31. <http://dx.doi.org/10.1016/j.coastaleng.2018.11.003>.
- [52] Camus P, Rueda A, Méndez FJ, Losada IJ. An atmospheric-to-marine synoptic classification for statistical downscaling marine climate. *Ocean Dyn* 2016;66(12):1589–601. <http://dx.doi.org/10.1007/s10236-016-1004-5>.
- [53] Rueda A, Camus P, Tomás A, Vitousek S, Méndez F. A multivariate extreme wave and storm surge climate emulator based on weather patterns. *Ocean Model* 2016;104:242–51. <http://dx.doi.org/10.1016/j.ocemod.2016.06.008>.
- [54] Camus P, Méndez F, Medina R. A hybrid efficient method to downscale wave climate to coastal areas. *Coast Eng* 2011b;58(9):851–62. <http://dx.doi.org/10.1016/j.coastaleng.2011.05.007>.
- [55] Camus P, Méndez FJ, Medina R, Tomás A, Izaguirre C. High resolution down-scaled ocean waves (DOW) reanalysis in coastal areas. *Coast Eng* 2013;72:56–68. <http://dx.doi.org/10.1016/j.coastaleng.2012.09.002>.
- [56] Gouldby B, Méndez F, Guanche Y, Rueda A, Mínguez R. A methodology for deriving extreme nearshore sea conditions for structural design and flood risk analysis. *Coast Eng* 2014;88:15–26. <http://dx.doi.org/10.1016/j.coastaleng.2014.01.012>.
- [57] Lara J, Losada I, Guanche R. Wave interaction with low-mound breakwaters using a RANS model. *Ocean Eng* 2008;35(13):1388–400. <http://dx.doi.org/10.1016/j.oceaneng.2008.05.006>.
- [58] Losada IJ, Lara JL, Guanche R, Gonzalez-Ondina JM. Numerical analysis of wave overtopping of rubble mound breakwaters. *Coast Eng* 2008;55(1):47–62.
- [59] Di Paolo B, Lara JL, Barajas G, Losada I. Wave and structure interaction using multi-domain couplings for Navier–Stokes solvers in OpenFOAM®. Part I: Implementation and validation. *Coast Eng* 2021;103799. <http://dx.doi.org/10.1016/j.coastaleng.2020.103799>.
- [60] Toimil A, Losada IJ, Díaz-Simal P, Izaguirre C, Camus P. Multi-sectoral, high-resolution assessment of climate change consequences of coastal flooding. *Clim Change* 2017;145(3). <http://dx.doi.org/10.1007/s10584-017-2104-z>.
- [61] Toimil A, Díaz-Simal P, Losada IJ, Camus P. Estimating the risk of loss of beach recreation value under climate change. *Tour Manag* 2018;68:387–400. <http://dx.doi.org/10.1016/j.tourman.2018.03.024>.
- [62] The-Rock-Manual. The rock manual. In: *The use of rock in hydraulic engineering*. 2nd ed.. London: CIRIA; 2007, p. 1175.
- [63] EurOtop. Manual on wave overtopping of sea defences and related structures. In: *An overtopping manual largely based on European research, but for worldwide application*. 2nd ed.. 2018, www.overtopping-manual.com.
- [64] ROM:31-99. Spanish recommendations for maritime port configuration design: Approach channel and harbour basin. Puertos del Estado; 1999, URL <http://www.puertos.es/es-es/ROM/Paginas/ROM-widisp.aspx>.
- [65] Thoresen CA. Port designer's handbook: Recommendations and guidelines. Thomas Telford Publishing; 2003, <http://dx.doi.org/10.1680/pdhrag.32286>.
- [66] Technical-Standards-For-Port-And-Harbour-Facilities-In-Japan. Technical standards and commentaries for port and harbour facilities in Japan (english edition). Overseas Coastal Area Development Institute of Japan. Ministry of Land, Infrastructure and Transport (MLIT); 2009.
- [67] Camus P, Méndez F, Medina R, Cofiño A. Analysis of clustering and selection algorithms for the study of multivariate wave climate. *Coast Eng* 2011a;58(6):453–62. <http://dx.doi.org/10.1016/j.coastaleng.2011.02.003>.
- [68] Díaz-Hernandez G, Rodríguez Fernández B, Romano-Moreno E, L. Lara J. An improved model for fast and reliable harbour wave agitation assessment. *Coast Eng* 2021;170:104011. <http://dx.doi.org/10.1016/j.coastaleng.2021.104011>.
- [69] Díaz-Hernandez G, Méndez F, Losada I, Camus P, Medina R. A nearshore long-term infragravity wave analysis for open harbours. *Coast Eng* 2015;97:78–90. <http://dx.doi.org/10.1016/j.coastaleng.2014.12.009>.
- [70] Sørensen JD, Burcharth HF. Reliability analysis of geotechnical failure modes for vertical wall breakwaters. *Comput Geotech* 2000;26(3):225–45. [http://dx.doi.org/10.1016/S0266-352X\(99\)00040-3](http://dx.doi.org/10.1016/S0266-352X(99)00040-3).
- [71] Goda Y. New wave pressure formulae for composite breakwaters. 1974, p. 1702–20. <http://dx.doi.org/10.1061/9780872621138.103>.
- [72] Tanimoto K, Takahashi S. Design and construction of caisson breakwaters — the Japanese experience. *Coast Eng* 1994;22(1):57–77. [http://dx.doi.org/10.1016/0378-3839\(94\)90048-5](http://dx.doi.org/10.1016/0378-3839(94)90048-5), Special Issue Vertical Breakwaters.
- [73] Sainflou G. Essai sur les digues maritimes verticales. *Ann Ponts Chaussées* 1928;98(tome II):5–48, 1928 (4).
- [74] Oumeraci H, Kortenhaus A, Allsop W, de Groot M, Crouch R, Vrijling H, Voortman H. Probabilistic design tools for vertical breakwaters. CRC Press; 2001.
- [75] van der Meer J. Rock slopes and gravel beaches under wave attack. 1988.

- [76] van Gent MR, van der Werf IM. Influence of oblique wave attack on wave overtopping and forces on rubble mound breakwater crest walls. *Coast Eng* 2019;151:78–96. <http://dx.doi.org/10.1016/j.coastaleng.2019.04.001>.
- [77] Tang G, Wang W, Song X, Guo Z, Yu X, Qiao F. Effect of entrance channel dimensions on berth occupancy of container terminals. *Ocean Eng* 2016;117:174–87. <http://dx.doi.org/10.1016/j.oceaneng.2016.03.047>.
- [78] Bouma JJ, François D, Schram A, Verbeke T. Assessing socio-economic impacts of wave overtopping: An institutional perspective. *Coast Eng* 2009;56(2):203–9. <http://dx.doi.org/10.1016/j.coastaleng.2008.03.008>, The CLASH Project.
- [79] Zerbe RO, editor. In: *Benefit-cost analysis*, Vol. Two volume set, Edward Elgar Publishing; 2008.
- [80] Abdelhafez MA, Ellingwood B, Mahmoud H. Vulnerability of seaports to hurricanes and sea level rise in a changing climate: A case study for mobile, AL. *Coast Eng* 2021;167:103884. <http://dx.doi.org/10.1016/j.coastaleng.2021.103884>.
- [81] Roebeling P, Coelho C, Reis E. Coastal erosion and coastal defense interventions: a cost-benefit analysis. *J Coast Res* 2011;1415–9.
- [82] Lima M, Coelho C, Veloso-Gomes F, Roebeling P. An integrated physical and cost-benefit approach to assess groins as a coastal erosion mitigation strategy. *Coast Eng* 2020;156:103614. <http://dx.doi.org/10.1016/j.coastaleng.2019.103614>.
- [83] Haasnoot M, Kwakkel JH, Walker WE, Maat JT. Dynamic adaptive policy pathways: A method for crafting robust decisions for a deeply uncertain world. *Glob Environ Change* 2013;23(2):485–98.
- [84] Walker WE, Haasnoot M, Kwakkel JH. Adapt or perish: A review of planning approaches for adaptation under deep uncertainty. *Sustainability* 2013;5(3):955–79.